Navidad development in the southern Bay of Biscay: Climate change and swoddy structure from remote sensing and in situ measurements

Carlos Garcia-Soto

Centro Oceanográfico de Santander, Instituto Español de Oceanografía (IEO), Ministerio de Ciencia y Tecnología (MCyT), Santander, Spain

Robin D. Pingree[1]

Institute of Marine Sciences (IMS), Plymouth University, Plymouth, UK

Luis Valdés

Centro Oceanográfico de Santander, Instituto Español de Oceanografía (IEO), Ministerio de Ciencia y Tecnología (MCyT), Santander, Spain

Received 5 June 2001; revised 31 January 2002; accepted 11 February 2002; published 30 August 2002.

[1] The warm water extension of the Iberian Poleward Current off northern Spain (''Navidad'') was examined in the advanced very high resolution radiometer (AVHRR) satellite archive (1979–2000) and in a time series of January sea surface temperatures. Winter warming in the southern Bay of Biscay during Navidad years was correlated with low values of the North Atlantic Oscillation (NAO) Index for the preceding months (November–December). Exceptional Navidad development and winter warming were observed during January 1990, January 1996, and January 1998, and extensive measurements were gathered for these 3 years. The Eastern Boundary poleward warming was found to extend from Portugal to Norway in exceptional Navidad years. The long-term changes of SST in the Navidad region (1967–2000) were analyzed in the frame of the decadal variation for the Celtic shelf (1890–2000), which showed an increase of 1°C over the century. During January 1990 and January 1996, cloud-free images of Navidad showed a pronounced production of slope water oceanic eddies (swoddies) in the SE corner of the Bay of Biscay. The small-scale properties of one of these swoddies (F90) were analyzed during summer from measurements at sea (RRS *Discovery* 193 cruise; July 1990). SeaSoar sections showed the physical structure of the swoddy core. The distribution and abundance of chlorophyll *a* associated with the swoddy was determined. It is shown that a swoddy has a higher chlorophyll *a* maximum in the seasonal thermocline than associated cyclones. Simultaneous satellite observations of the sensors AVHRR, Sea-viewing Wide Field-of-view Sensor (SeaWiFS), and altimeter (combined TOPEX/Poseidon/ERS-2 data) were used to analyze the remote sensing properties of three summer swoddy-like eddies during August 1998. The summer SeaWiFS chlorophyll *a* concentration at the center of the eddy near 45.5°N, 6°W (AE6) was appraised against a time series (September 1997 to April 2001) of SeaWiFS chlorophyll *a* concentration representative of a central region of the Bay of Biscay. *INDEX TERMS:* 1635 Global Change: Oceans (4203); 4215 Oceanography: General: Climate and interannual variability (3309); 4516 Oceanography: Physical: Eastern boundary currents; 4520 Oceanography: Physical: Eddies and mesoscale processes; 9325 Information Related to Geographic Region: Atlantic Ocean; *KEYWORDS:* Eastern Boundary Current, SST, eddy, Bay of Biscay, chlorophyll *a*

1. Introduction

[2] Infrared satellite images of the Advanced Very High Resolution Radiometer (AVHRR) have shown in recent years the existence of a warm surface current circulating poleward along the Iberian slopes of the NE Atlantic [*Pingree and Le Cann*, 1989, 1990; *Haynes and Barton*, 1990; *Frouin et al.*, 1990]. The phenomenon is now considered a common feature of the winter circulation of eastern oceanic margins known as Eastern Boundary Currents (EBC) [*Neshyba et al.*, 1989]. As the Poleward Current off the Iberian Peninsula enters the Bay of Biscay around Cape Finisterre (NW Spain), warm water moves eastward along

[1]Also at Marine Biological Association of the United Kingdom (MBA), Citadel Hill, Plymouth, UK.

0148-0227/02/2001JC001012

the Cantabrian continental shelf and slope (see, for example, Figure 1); some flow continues its poleward advance across the Landes Plateau and the continental slope of Cap Ferret canyon. The January warm water extension of the Iberian Poleward Current (IPC) along the Cantabrian region has been referred to as Navidad (Christmas) as it starts to be conspicuous near Christmas and New Year. A relevant characteristic of the poleward flow is its inability to follow the abrupt changes of topography, such as Cape Ortegal and Cap Ferret Canyon [*Pingree and Le Cann*, 1989, 1990]. At these locations, the slope water is injected into the oceanic region to form anticyclonic eddies that contain a core of slope water. These slope water oceanic eddies (or swoddies) are surface warm features, and therefore it has been possible in the past to determine from infrared satellite images their date and place of birth and to follow their movements in the Bay of Biscay [*Pingree and Le Cann*, 1992a]. During summer, when the summer thermocline caps the eddy core, swoddies can be identified in infrared satellite images from the sea surface cooling that results from the doming of the seasonal thermocline above the swoddy core [*Pingree and Le Cann*, 1992a] (see also Figure 2).

[3] During the winter 1989/1990, particularly strong Navidad conditions resulted in the production of 3 marked swoddies. One of the swoddies (F90) was shed into the ocean near Cap Ferret canyon and was tracked by AVHRR across the southern Bay of Biscay over a 9 month period. This swoddy was surveyed in July on *Discovery* cruise 193 [*Pingree and Le Cann*, 1992a]. The authors showed temperature, salinity and density sections of F90 using SeaSoar, XBTs, and CTDs. Velocity distributions were derived from CTDs, ADCP and drogued Argos buoys. More investigations of similar eddies (termed swoddy-like eddies as their slope water origin could not be established from AVHRR imagery) were carried out in September 1991 [*Pingree and Le Cann*, 1992b] and in April 1992 [*Pingree*, 1994a], where Lagrangian properties were derived from the deployment of drogued buoys.

[4] The present paper centers on the analysis of long-term observations of Navidad and swoddy or swoddy-like structures, and a description of the properties of these eddies from recent satellite observations and cruise measurements. In the first part of the study (section 3.1), the interannual variability of Navidad is described from the long-term archive of AVHRR satellite images (1979–2000) in conjunction with a time series of January Sea Surface Temperatures (1967–2000) (section 3.1.1). Poleward winter warming is also analyzed over a much larger extent of the N Atlantic Eastern Boundary, from the Subtropical Front to the Polar Front, for the exceptional Navidad years 1990, 1996, and 1998 (sections 3.1.2 and 3.1.3). January winter warming is examined in relation to the North Atlantic Oscillation Index variability and the production of winter swoddies in the SE corner of the Bay of Biscay (sections 3.1.4 and 3.1.5). Some aspects of Navidad and poleward warming of climatic significance (decadal SST changes and winter warming heat flux along the continental slope margin) are finally addressed (sections 3.1.6 and 3.1.7).

[5] The second part of the work (section 3.2) describes first the distribution pattern of summer swoddy-like structures found in the southern Bay of Biscay between 1979 and 2000 (AVHRR archive) (section 3.2.1). The work overall covers remote sensing applications to the study of summer swoddy-like structures following two marked years of Navidad development, 1990 and 1998. The remote sensing signatures of the 1998 summer eddy structures are determined using simultaneous observations of AVHRR, altimeter and SeaWiFS data (sections 3.2.2 and 3.2.3). Field data (SeaSoar temperature and relative fluorescence profiles and ADCP measurements) from the summer survey of swoddy F90 are used to describe the in situ structure and small-scale properties of the eddy core and its exterior regions (sections 3.2.4, 3.2.5, and 3.2.6). It is shown that these measured physical characteristics largely determine the infrared, altimeter and surface SeaWiFS chlorophyll *a* remotely sensed eddy signatures.

[6] Comparable poleward flows and associated eddies have been described for other regions, for example, along the western continental slopes of Australia (SE Indian Ocean) [*Cresswell and Golding*, 1980; *Church et al.*, 1989; *Griffiths and Pearce*, 1985a, 1985b; *Pearce and Griffiths*, 1991], and so the results presented are likely to have a wider significance than for the region investigated (North Atlantic Ocean, Eastern Boundary).

2. Methods

[7] AVHRR satellite data used for long-term observations (1979–2000) of Navidad development and eddy structure were received and processed (as enhanced channel 4 images) at the Dundee Satellite Receiving Station (DSRS) [e.g., *Dickson and Hughes*, 1981]. Some characteristics of the images used (date, GMT overhead time, NOAA satellite number, orbit and identification code of Dundee University) are given in Tables 1a (Navidad) and 1b (summer eddies). More detailed studies of Navidad and summer eddy structure were undertaken on AVHRR data received at DSRS (http://www.sat.dundee.ac.uk) and at the University of Las Palmas de Gran Canaria (ULPG); processing to enhanced channel 4 or SST images was carried out at IEO following standard AVHRR image analysis techniques [e.g., *Holligan et al.*, 1989]. A large-scale analysis of January 1990 sea surface

Figure 1. (opposite) Thermal infrared satellite images (AVHRR, channel 4) showing the warm Iberian slope current entering the Bay of Biscay around Galicia (NW Spain) and extending along the Cantabrian shelf and slopes during the winters of (a) 1997/1998 (08.01.98), (b) 1995/1996 (18.01.96), (c) 1989/1990 (12.01.90), (d) 1987/1988 (11.01.88 and 19.01.88), (e) 1983/1984 (28.12.83), (f) 1981/1982 (17.01.82), and (g) 1978/1979 (17.01.79). These late December–January images represent the most pronounced observations of Navidad in the historical archive of AVHRR satellite images of the Bay of Biscay (1979–2000). Annotations in Figure 1c show Navidad warm water being shed from the French slopes into the oceanic SE Bay of Biscay during the winter 1989/1990. These warm water instabilities gave birth to slope water oceanic eddies F90 and F90b from near Cap Ferret canyon. Swoddy O90 (also shown) was born from a projection of Navidad warm water near Cape Ortegal (8°W).

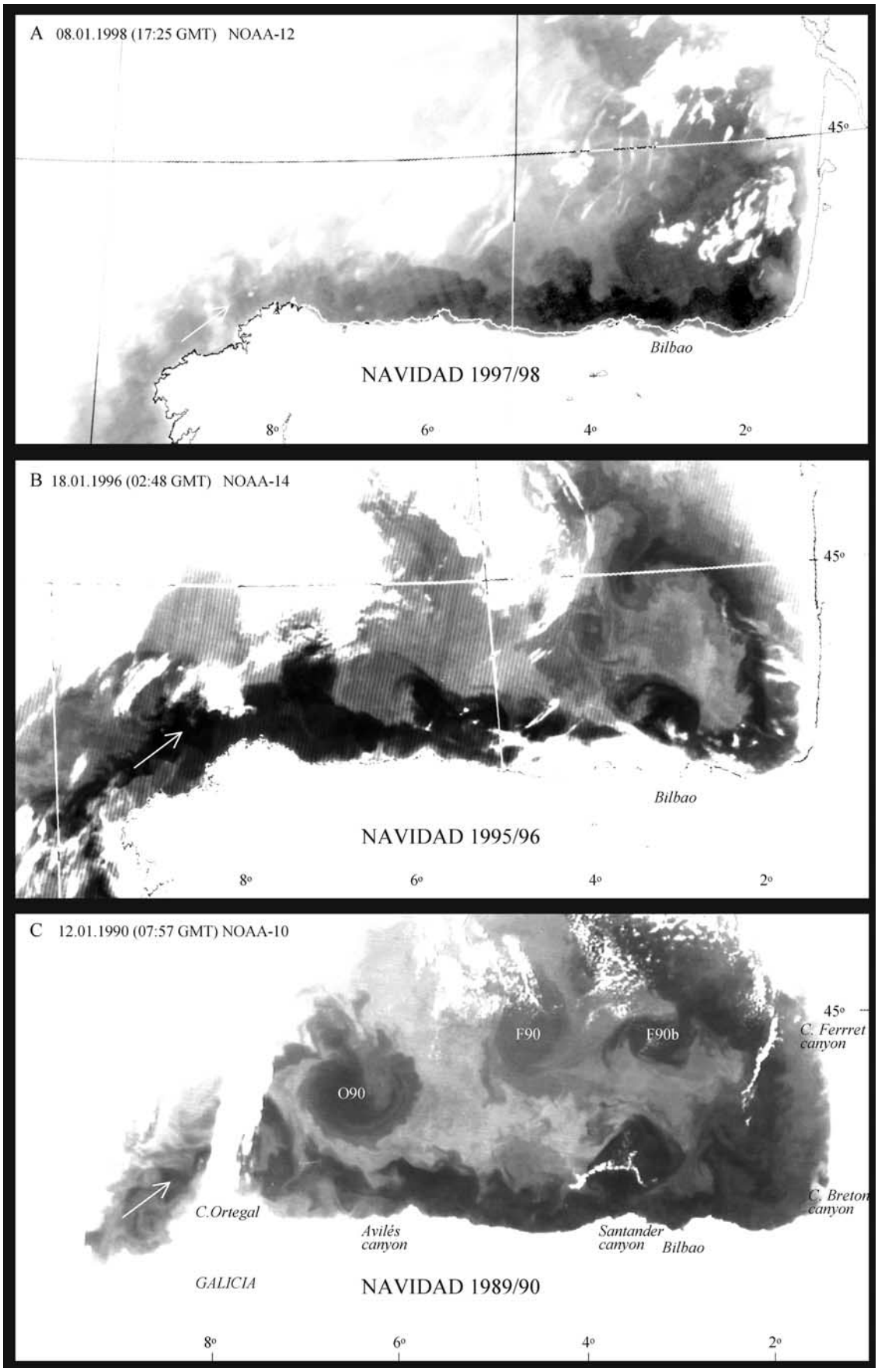
A 08.01.1998 (17:25 GMT) NOAA-12
45º
Bilbao
NAVIDAD 1997/98
8º
6º
4º
2º
B 18.01.1996 (02:48 GMT) NOAA-14
45º
Bilbao
NAVIDAD 1995/96
8º
6º
4º
2º
C 12.01.1990 (07:57 GMT) NOAA-10
45º
F90
F90b
C. Ferrret canyon
O90
C. Breton canyon
C.Ortegal
Avilés canyon
Santander canyon
Bilbao
GALICIA
NAVIDAD 1989/90
8º
6º
4º
2º

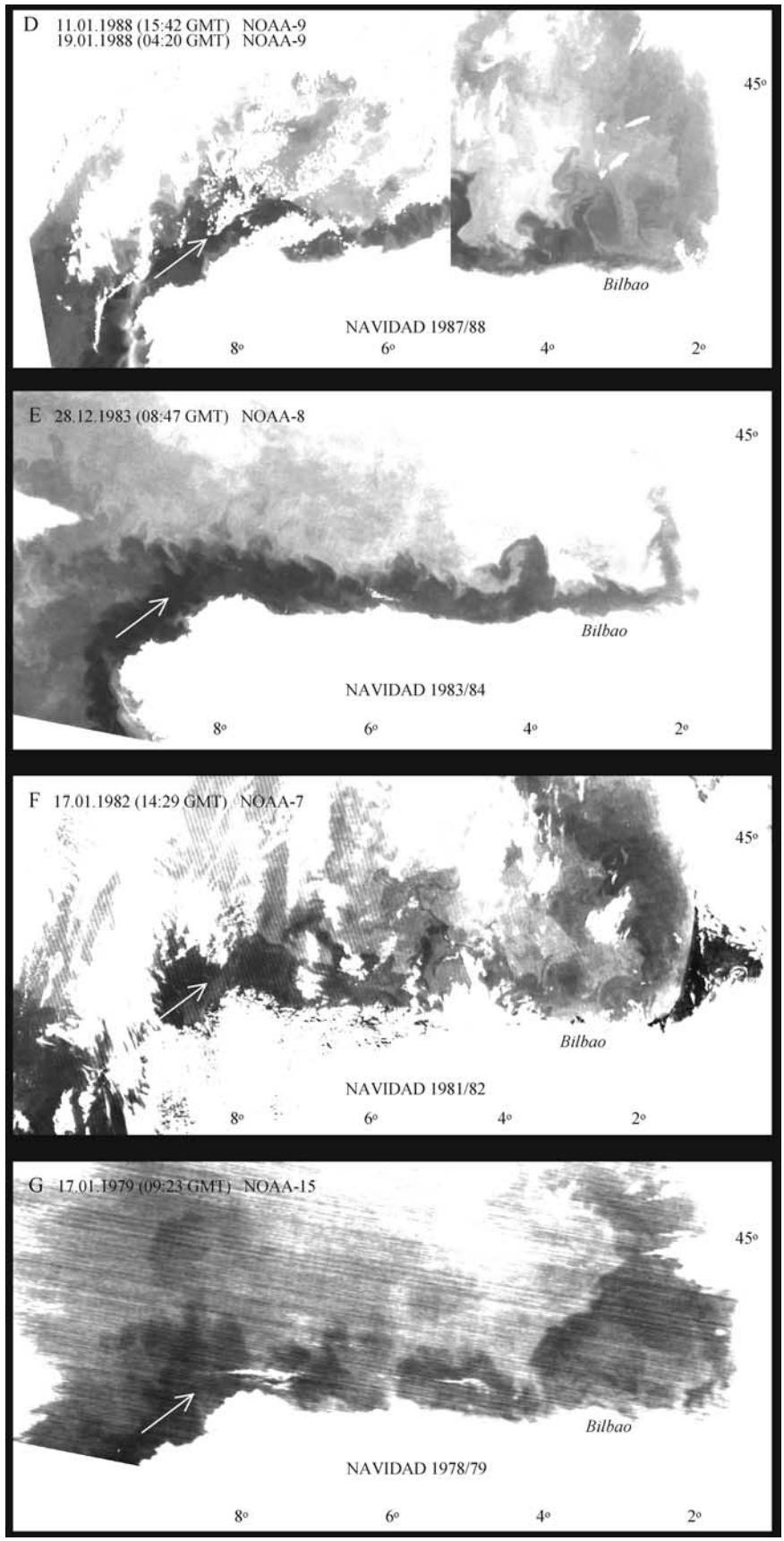

Figure 1. (continued)

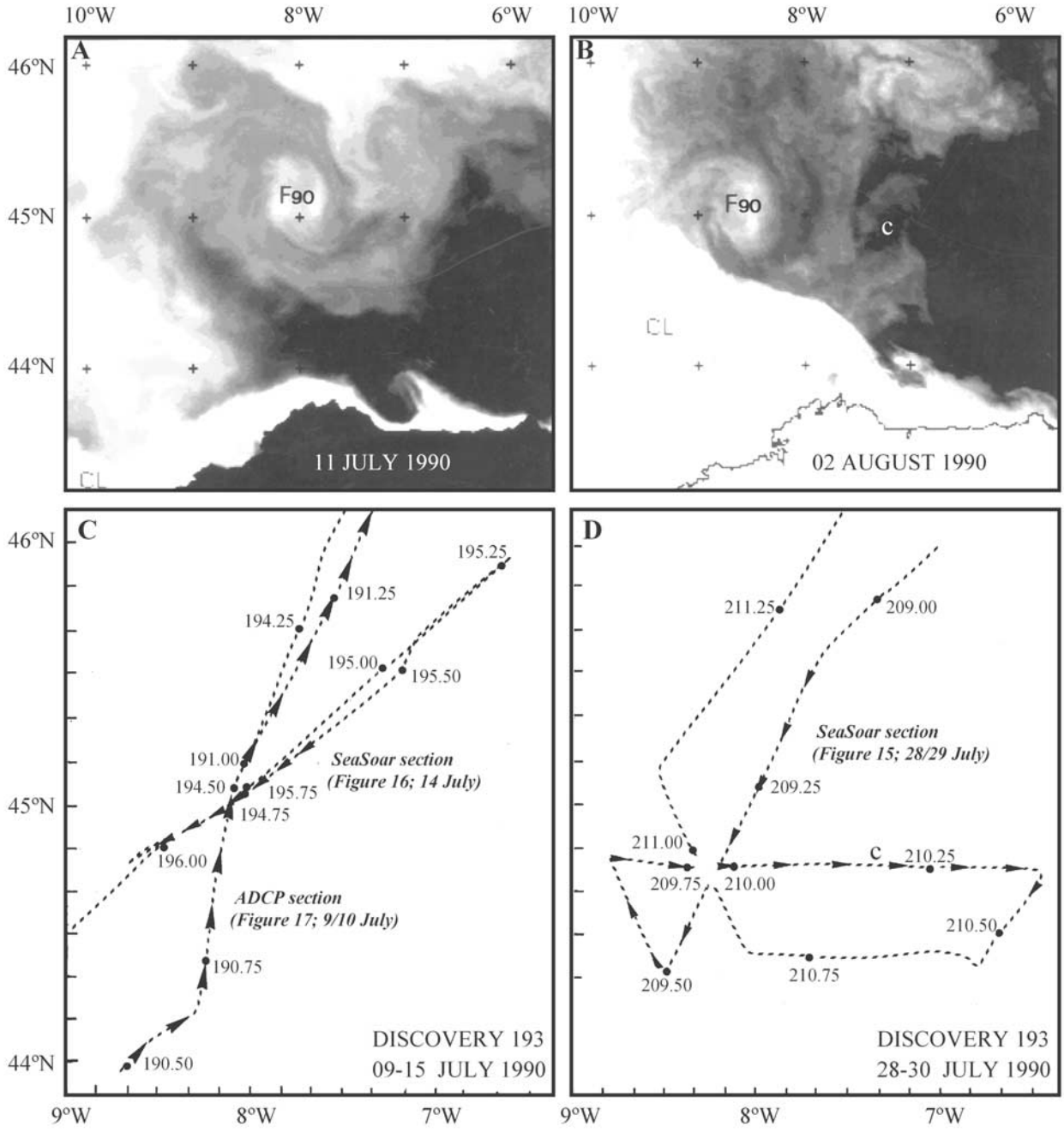

Figure 2. AVHRR thermal infrared satellite images showing swoddy F90 on (a) 11 July 1990 (1328 GMT) and (b) 02 August 1990 (0254 GMT). The change of position of the eddy center (observed as a surface cool patch due to doming of the seasonal thermocline) gives a mean westward translation velocity of $\sim$1.7 cm s^{-1} over this 22 d period. C indicates a cyclone associated with F90. Summer upwelling off NW Spain is evident as cool coastal waters (white shades); Cl (also in white) indicates cloud cover. The warmer water to the north of the upwelling is also moving westward in the vicinity of the continental slope because of the rotation influence of the eddy. (c) Tracks of *Discovery* cruise 193 that surveyed swoddy F90 during 9–15 July 1990 and (d) 28–30 July 1990. Time along the cruise track is annotated with decimal yearday (1990), which fixes the SeaSoar and ADCP sections illustrated in Figures 15, 16, and 17. During the second survey, the cyclone associated with F90 was also cut by the cruise track, and a C annnotation indicates a central position.

temperatures was carried out on AVHRR data processed at the Centre of Space Meteorology at Lannion [e.g., *CMS*, 1992]; to examine poleward along-slope SST anomalies, the data were reprojected at IEO against the GEBCO bathymetric data base [*British Oceanographic Data Centre* (*BODC*), 1997]. SeaWiFS and altimetric satellite data for a 1998 eddy study were received and processed respectively at the University of Santiago and at the CLS Space Oceanography Division (the later as part of the EU Projects AGORA and DUACS). The summer 1998 satellite data (IR, SeaWiFS, and altimeter) were selected to coincide with the period of R/V *Professor Shtokman* cruise 8/98, which investigated a summer swoddy-like structure in August 1998 (E. Fernández et al., The planktonic biology of a slope water anticyclonic eddy (swoddy) in the southern Bay of Biscay, submitted to *Deep-Sea Research*, 2002, hereinafter referred to as Fernández et al., submitted manuscript, 2002). Processing of SeaWiFS data to final chlorophyll *a* concentration (C_a) used the SeaDAS software, and estimated C_a from the ratio of radiances measured in band 3 (480–500 nm) and band 5 (545–565 nm) according to the following NASA algorithm: $C_a = \exp [0.464 - 1.989 \text{ Ln } (L_{WM}490/L_{WM}555)]$. The analysis of altimeter data (combined TOPEX/Poseidon/ERS-2) to a final sea level anomaly (SLA) map followed *Le Traon and Ogor* [1998]. The sea level anomalies were relative to a 3 year mean (January 1993 to January 1996) with a spatial interpolation to 0.25° latitude × 0.25° longitude and a temporal resolution of 10 days. Instrumental noise is about 2cm RMS (T/P) and 3cm RMS (ERS-2). A time series (1997–2001) of SeaWiFS chlorophyll *a* concentration showing Spring and Autumn bloom development in the Bay of Biscay was undertaken at the Institute of Marine Science (University of Plymouth); data were provided by the NASA Distributed Active Archive Centre (DAAC/GSFC).

[8] A time series of sea surface temperature (SST) in the Navidad region extends a previous time series by *Pingree and Le Cann* [1992b] (1984–1991 data) and *Pingree* [1994a] (1967–1993 data) and uses the same data sources [e.g., *Centre de Météorologie Spatiale* (*CMS*), 1992] for the remaining 1994–2000 period. A SST time series in the Celtic Shelf extends a previous ~75 y time series (1903–1974) by *Pingree* [1980] (Seven Stones Lightship station, in a region of tidally mixed water; ~75m depth) and also uses CMS/CMM data for the last ~25 year period (1975–1999). Standardized monthly values of the North Atlantic Oscillation Index (NAO) were extracted from the Climate Prediction Centre (NOAA-CPC; USA). The CPC diagnostic procedure is the Rotated Principal Component Analysis (RPCA) [*Barston and Livezey*, 1987] that isolates the primary teleconnection patterns for all months and allows for time series of the amplitudes of the patterns to be constructed. Records of NAO available at CPC date back to 1950; records of NAO dating back to 1824 are shown for example by *Visbeck et al.* [2001] in CLIVAR Exchanges Newsletter 6 (1). An extensive white paper reviewing Atlantic Climate Variability and NAO in the context of CLIVAR [e.g., *Kushnir*, 1994; *Hurrell*, 1995, 1996; *Dickson et al.*, 1996; *Dickson*, 1997] can be found in http://geoid.mit.edu/accp/avehtml.html [see also *Marshall et al.*, 2001]. SeaSoar and ADCP data representing swoddy structure were taken from the two surveys of *Discovery* cruise 193 (09–15 July 1990 and 28–30 July 1990). Cruises for other data used in this work (CTDs and XBTs) and the related published studies are shown in Table 1b. SeaSoar relative fluorescence units (*Discovery* 193 cruise) were changed to chlorophyll *a* levels (mg m^{-3}) using two values at the eddy center (~0.3 mg m^{-3} at surface and 0.8 mg m^{-3} at 35 m) to give an indication of overall levels; the values given are only used in a relative sense. Representative July surface values of chlorophyll *a* (~0.3 mg m^{-3}) for the Bay of Biscay near 47°N are given by *Garcia-Soto and Pingree* [1998]. Seasonal SeaWiFS values representing the Bay of Biscay (45°/46°N) are given in this paper. A summary of the main hydrological structures in the Bay of Biscay are given by *Koutsikopoulos and Le Cann* [1996].

3. Results and Discussion

3.1. Navidad Development and Climate Change

3.1.1. Navidad Interannual Variability

[9] IR images of the Bay of Biscay during late December–January were examined and appraised for the period 1979–2000 in order to analyse the interannual variability of Navidad. The particular dates of the cloud-free images found in the archive are shown in Table 1a, and the most marked IR observations of Navidad occurrence are presented in Figure 1. Satellite observations of marked Navidad showed the warm water structure from the Iberian Poleward Current (IPC) stretching along the whole extent of the Cantabrian shelf and slopes. Cloud-free images of this type were found for the winters 1979, 1982, 1984, 1988, 1990, 1996, and 1998, adding 2 more years (1996 and 1998) to a previous remote sensing appraisal up to 1991 [*Pingree and Le Cann*, 1992a]. Years without a Navidad influence could still show IPC warm water turning eastward around Galicia though a clear warm water structure was not present along the Cantabrian shelf/slopes; these type of images were found during January 1983, 1987, 1997, 1999, and 2000. The rest of the cloud-free observations in the AVHRR archive (years 1986, 1989, 1991, 1992, 1993, 1994, and 1995) were considered as of weak Navidad influence; in these type of images a pronounced warm water region did not extend eastward generally further than ~6°W (near Aviles canyon).

[10] To examine a cause for Navidad interannual variability, we compared the North Atlantic Oscillation Index (NAO) for November–December (Figure 3a) with January Sea Surface Temperatures observed along the north Spanish continental slopes (8°W to 4°W; Figure 3b). NAO represents the first mode (32% of variance) of low frequency variability over the North Atlantic [*Cayan*, 1992a] and its regional extension and amplitude is most pronounced during the winter (December–February) [*Barston and Livezey*, 1987], near the period of Navidad development. Some lag between January SST off northern Spain at 4°W and NAO would also be expected. The slope current has typical winter values of 10–20 cm s^{-1} so an advective influence from the Iberian slope might take a month or two to reach the SE corner of the Bay of Biscay. NAO data for November–December were extracted from ftp://ftp.ncep.noaa.gov/pub/cpc/wd52dg/data/indices/tele_index. nh. No clear relationship was found between NAO and SST values for the whole data set, both when including (1967–2000; $r^2 = 0.12$ at 4°W

Table 1a. Summary of Characteristics of AVHRR Satellite Images (Enhanced Channel 4) From Dundee University Used for Long-Term (1979–2000) Observations of Navidad Development (Figure 1)[a]

Date	Time	NOAA	Orbit	DSRS ID	Navidad Development	Published Navidad Images
17.01.79	0923	N-5	11161	164/07	marked Navidad	see Figure 1
17.01.80					obscured by cloud (obc)	
17.01.81					obc	
17.01.82	1429	N-7	2937	333/01A	marked Navidad	see Figure 1
08.01.83	1411	N-7	7963	3821/01B	no Navidad structure	
28.12.83	0847	N-8	3904	435/06B	marked Navidad	*Pingree and Le Cann* [1989]; see Figure 1
28.12.85					obc	
09.01.86	0250	N-9	5538	570/12A	weak Nvidad	
05.01.87	0345	N-9	10631	640/13B	no Navidad structure	
11.01.88	1542	N-9	15872	711/07B	marked Navidad	see Figure 1
19.01.88	0420	N-9	15978	712/12B		
29.01.89	0853	N-10	12294	789/01A	weak Navidad	*Pingree and Le Cann* [1992b]
12.01.90	0757	N-10	17243	855/01B	marked Navidad	*Pingree and Le Cann* [1990]; see Figure 1
					warm water seen extending along slopes from Portugal to Shetland Isles	see Figure 4
12.01.91	0305	N-11	11971	926/01B	weak Navidad	
06.01.92	0309	N-11	16911	1117/06	weak Navidad	
22.01.93	0827	N-12	8792	1259/12	weak Navidad	
18.01.94	1603	N-11	27410	1397/13	weak Navidad	
13.01.95	0946	N-9	52004	1531/09	weak Navidad	
18.01.96	0248	N-14	5413	1684/10	marked Navidad	see Figure 1
					slope current continuity from Celtic Sea to North Sea shown by the buoy track	see Figure 6
15.01.97	1357	N-14	10541	1887/01	no Navidad structure	
08.01.98	1725	N-12	34559	2100/11	marked Navidad	see Figure 1
12.01.98	0317	N-14	15642	2102/09	warm water seen extending along slopes from Portugal to Shetland Isles	see Figure 5
12.01.98	0317	N-14	15642	2102/09		
19.01.98	0341	N-14	15741	2106/09		
21.01.98	0319	N-14	15769	2107/11		
22.01.98	0308	N-14	15783	2108/05		
30.01.99	1432	N-14	21053	2522/12	no Navidad structure	
05.01.00	0424	N-14	25845	2522/12	no Navidad structure	

[a] The 1979–2000 most clear observations of Navidad development in late December/January (Figure 1).

and $r^2 = 0.17$ at 8°W) or excluding (1972–2000; $r^2 = 0.12$ at 4°W and $r^2 = 0.15$ at 8°W) the sparse ICES data. A selective comparison limited to the years of marked satellite-observed Navidad (see year annotations in Figure 3b) showed on the other hand that the SST values at 4°W and 8°W were tightly associated ($r^2 = 0.95$ at 4°W and $r^2 = 0.97$ at 8°W) with low values (∼negative) of the N–D NAO Index (Figures 3c and 3d), or negatively correlated with N–D NAO. January 1996, for example, with the highest January temperature on record (15°C), was preceded (in November–December 1995; 1996 as year + 1) by the lowest NAO value over the last 50 years.

[11] A relationship between negative NAO and positive SST anomalies during winter in the North Atlantic has been attributed to decreasing wind speed in the negative phase of NAO and associated decrease of latent and sensible heat fluxes [*Cayan*, 1992a, 1992b]. At a more regional scale, we can only speculate on the cause for a relationship between warm water off NW Spain and a negative NAO index. In the negative phase of NAO, the northerly component of wind stress might relax or reverse allowing water near the surface in the vicinity of the Iberian continental slope to move poleward. Some IR images also show a warm source of winter water as far south as the Tagus Abysal Plain. A branch or northern recirculation of the eastern extension of the Azores Current can flow north toward the Iberian Peninsula [*Pingree*, 1997], and we suggest a link between the winter Navidad and a northward branch of the Azores Current or subtropical water [*Pingree*, 2002].

3.1.2. The 1990 Winter Poleward Warming Over the Eastern Boundary of the North Atlantic

[12] As NAO is a large-scale atmospheric pressure pattern, we analyzed Navidad-like winter warming over a larger geographical region. Figure 4 shows the distribution of AVHRR sea surface temperature during January 1990 (an exceptional Navidad year) in the Eastern Boundary of the North Atlantic from 27°N (south of the Canary Islands) to 65°N (Iceland). The distribution is presented only for January 1990 as cloud coverage prevented much of the SST observations in the CMS archive north of ∼50°N and south of ∼40°N during the other exceptional Navidad years (January 1996 and January 1998). Figure 4 showed pulses of warm water (shaded regions) extending northward along the shelfbreak/slopes from the Subtropical Front (∼35°N) [*Pingree et al.*, 1999a] to near the Polar Front (Iceland-Faeroe Front; ∼62°N), establishing clearer than ever before the large-scale extent of winter poleward warming along the European continental slope margin.

[13] Previous regional observations of poleward warming/poleward current include investigations along the Iberian slopes [*Pingree and Le Cann*, 1989, 1990; *Frouin et al.*, 1990; *Haynes and Barton*, 1990; *Garcia-Soto et al.*, 1991; *Fiuza et al.*, 1998], the Cantabrian slopes [*Pingree and Le Cann*, 1989, 1990; *Urrutia and Garcia-Soto*, 1990;

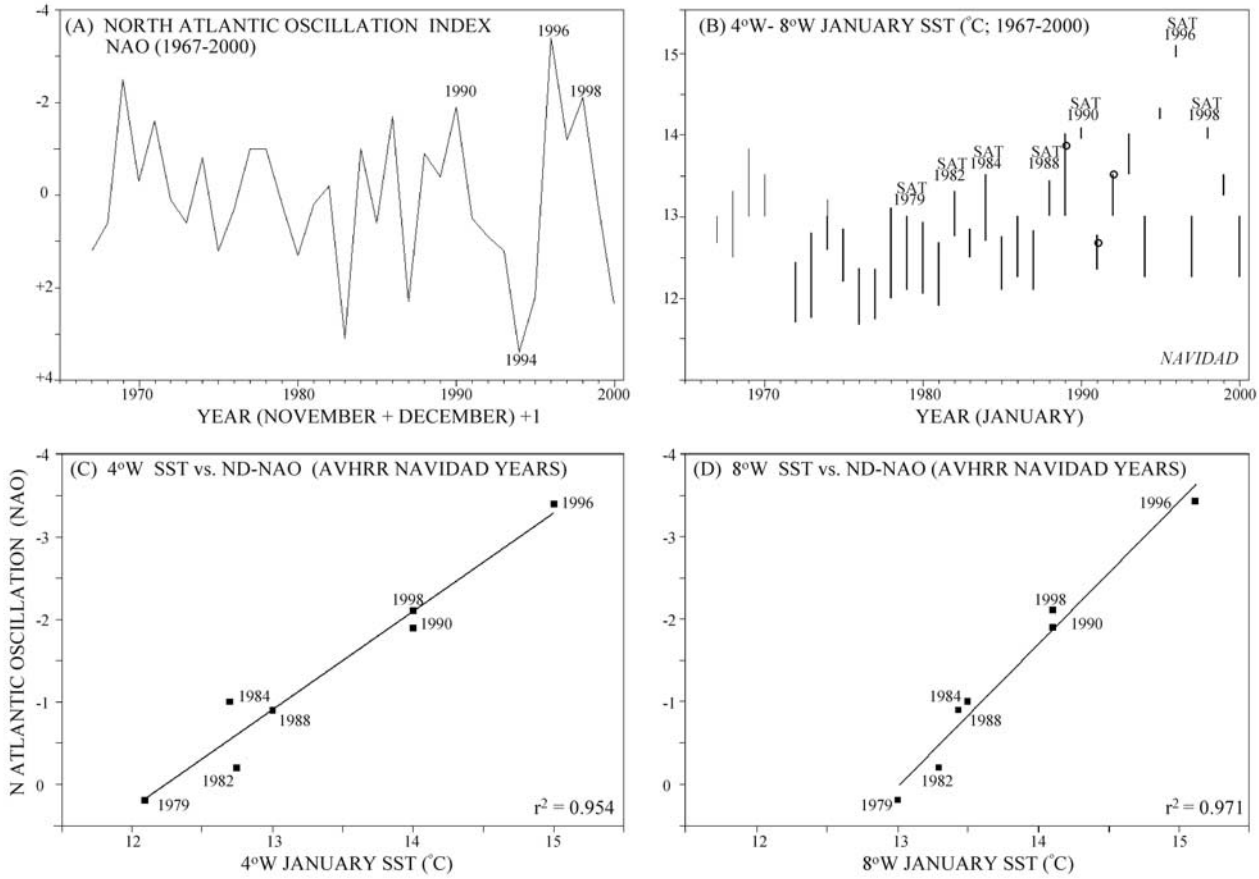

Figure 3. (a) November–December (N–D) values of the North Atlantic Oscillation (NAO) Index for the period 1965–2000. ''Year (November + December) + 1'' (see horizontal axis) indicates N–D NAO values the year preceding the January SST values given in Figure 3b. (b) January sea surface temperature (SST) for years 1967–2000 along the north Spanish slopes from about 8°W (upper value) to about 4°W (lower value). Thick lines (1972–2000) represent data obtained from CMM/CMS [e.g., *CMS*, 1992] and thin lines (1967–1970) data obtained from *International Council for the Exploration of the Sea* (*ICES*) [1971]. Circles [from *Pingree*, 1994a] are maximum temperatures from calibrated thermistors on current meters that show warm water penetrating to depths of ~200 m near 7°W. Year annotations indicate the years with late December–January observations of marked Navidad in the AVHRR archive (1979–2000) and shown here in Figure 1. Relationships between the N–D NAO Index and January SSTs (c) at 4°W and (d) at 8°W during the years of marked Navidad. Though the number of observations is low (n = 7) the distribution is tight and significant (r^2 = 0.95 at 4°W and r^2 = 0.97 at 8°W).

Fernández et al., 1993; *Pingree*, 1994a; *Sánchez and Gil*, 2000], the Armorican and Celtic slopes [*Pingree and Le Cann*, 1989; *Garcia-Soto and Pingree*, 1998], the Goban Spur region [*Pingree et al.*, 1999b], the Rockall Channel [*Dickson et al.*, 1986] and the West Shetland slopes [*Gould et al.*, 1985; *Pingree et al.*, 1999b]. In Figure 4, the slope water is about 1°C warmer than the adjacent ocean and shelf regions. In the central region, the surface temperature at Goban Spur is ~12.5°C or about ~1.5°C warmer than in January 1994, a weak Navidad year (~11°C (CMS); cf. ~11.25°C given by *Pingree et al.* [1999b]). The mean poleward temperature gradient along the continental slope margin is about −0.25°C per degree of latitude with a weakening poleward trend. The slope region considered is

Figure 4. (opposite) AVHRR sea surface temperature (°C) distribution during January 1990 showing pulses of warm water (shaded regions) extending northward along the shelfbreak/slope region of the NE Atlantic from ~35°N, near the Subtropical Front, to ~60°N, near the Polar Front; the 200 m and 2000 m depth contours are shown. S annotations along the 33°–34°N latitude indicate cool structures transferring cooler ENACW (Eastern North Atlantic Central Water) southward across the Subtropical Front boundary [see *Pingree et al.*, 1999a]. January 1990 was a year of exceptional Navidad development, and the extent of the 1990 Navidad is indicated by a double arrow (see Figure 1c). L denotes two regions (NW Spain and Goban Spur region) where the warm slope water is shed into the ocean because of the abrupt change of shelfbreak/slope orientation. Triangles show the locations in the shelfbreak/slope regions where a relationship between SST (January) and NAO (November–December) Index during Navidad years (1979, 1982, 1984, 1988, 1990, 1996, and 1998) was examined (see Figures 3 and 7).

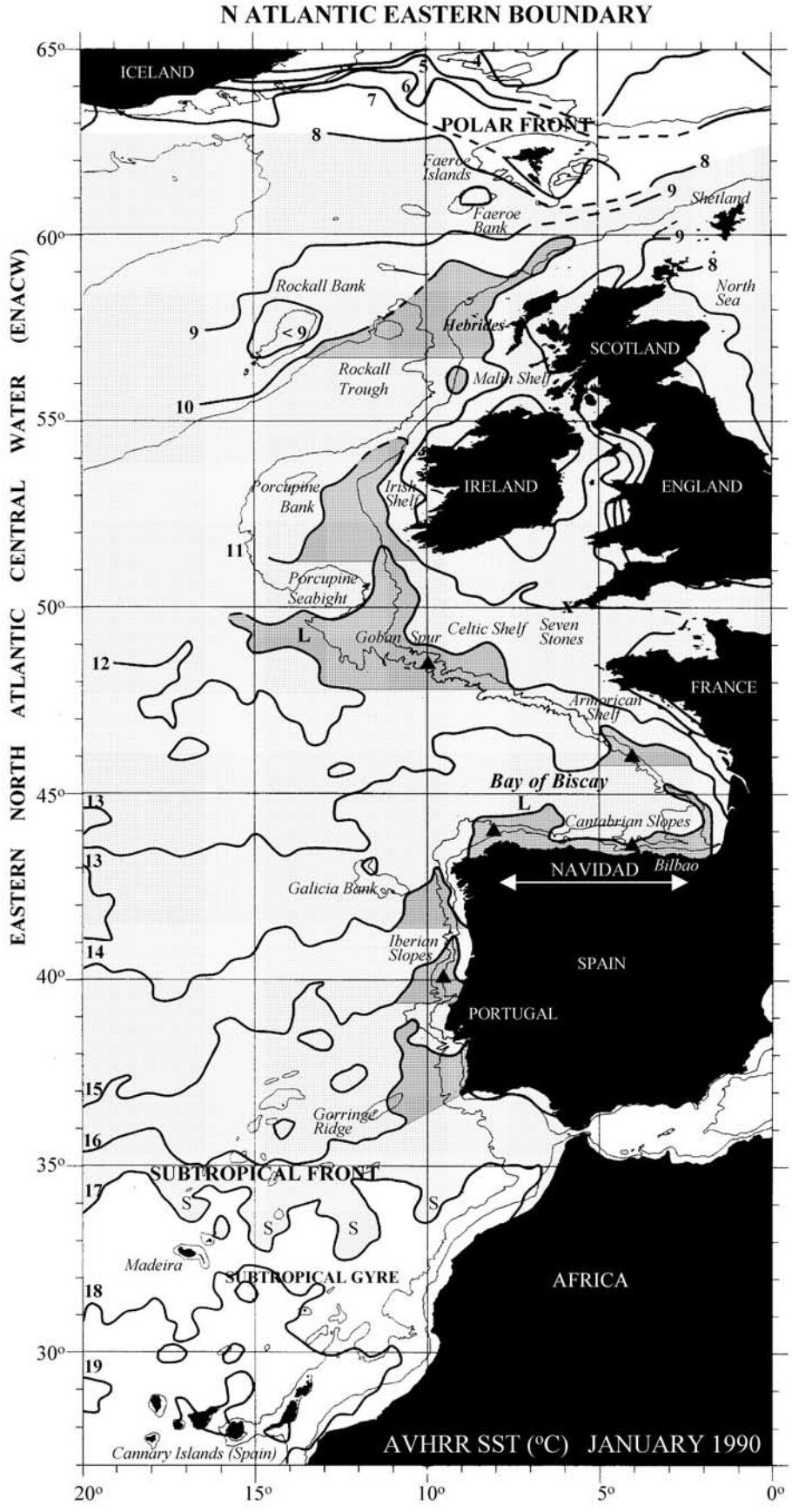
N ATLANTIC EASTERN BOUNDARY
EASTERN NORTH ATLANTIC CENTRAL WATER (ENACW)
ICELAND
POLAR FRONT
Faeroe Islands
Faeroe Bank
Shetland
North Sea
Rockall Bank
Hebrides
SCOTLAND
Rockall Trough
Malin Shelf
IRELAND
ENGLAND
Porcupine Bank
Irish Shelf
Porcupine Seabight
Goban Spur
Celtic Shelf
Seven Stones
FRANCE
Armorican Shelf
Bay of Biscay
Cantabrian Slopes
NAVIDAD
Bilbao
Galicia Bank
Iberian Slopes
SPAIN
PORTUGAL
Gorringe Ridge
SUBTROPICAL FRONT
Madeira
SUBTROPICAL GYRE
AFRICA
Cannary Islands (Spain)
AVHRR SST (ºC) JANUARY 1990
65º
60º
55º
50º
45º
40º
35º
30º
20º
15º
10º
5º
0º

about ~3000 km in extent so there is an average drop of about 1°C per 500 km following the poleward flow along the continental slope.

[14] Figure 4 also shows some aspects of the poleward warming/poleward flow associated to bathymetry (200–2000 m depths). The surface pulses have a more pronounced northward advance along the shelfbreak (200 m depth) in the Armorican shelf, Celtic shelf, Irish shelf and Hebrides shelf regions. In the Iberian region north of 39°N, where the shelf is narrower, the poleward advance of the warm pulses appear more associated to the slopes (200–2000 m depth). Along the Iberian slopes (36°–43°N) and the northern Celtic Sea-Irish shelf-break (49°–54°N), where the shelfbreak is orientated N/S, the poleward warm water pulses show a higher along-slope SST gradient. In the Cantabrian region where the shelf is orientated E-W, a poleward advance along the slopes is not longer possible and the warm water (14°C) spreads across the shelf (see also Figure 1c). Near NW Spain and in the Goban Spur region, where the shelfbreak changes direction markedly, some warm water is seen to leave the shelfbreak/slopes region and is projected into the deep ocean (see L annotations). Leakage (L) of slope water from Goban Spur during May (shelfbreak cooling water) has been described by *Pingree et al.* [1999b] who also analyzed the seasonality of the slope currents in this OMEX (Ocean Margin Exchange) study area. Leakage of warm slope water off NW Spain (where there is also an abrupt change of topographic direction) during January 1990 and the associated production of an slope water oceanic eddy (O90) can be seen in Figure 1c which shows the extent of the 1990 Navidad.

3.1.3. The 1996 and 1998 IR Observations and Measurements of Winter Poleward Warming/PolewardFlow

[15] During the winters 1995/1996 and 1997/1998, individual AVHRR satellite images from the DSRS archive also showed the presence of warm water associated with the continental slope margin despite generally overcast conditions. A relatively cloud-free region in January 1998 is shown here for the West Shetland Slope and Shelf (Figure 5a; 12 January) and the Iberian, Cantabrian and Armorican slopes (Figure 5b; 19, 21, and 22 January). The southern limit of the poleward warming in these images was also found near the Subtropical Front at 36°N with source waters for the Iberian slope sometimes collecting in the Tagus Abyssal Plain (but deeper water on the slope will contain Mediterranean Water in the undercurrent). To the north, shelfbreak/slope warm water pulses were observed up to 62°N, or along the Faeroe-Shetland Channel; warm winter water will enter the Northern North Sea north of the Shetlands and also continue on along the continental slope to Norway.

[16] A notable measurement of slope current continuity related to these observations is shown by the track of Argos Buoy 3350 during the winter 1995/1996 [*Pingree et al.*, 1999b]. The buoy track is also shown here (Figure 6) in relation to the COADS SST distribution during January 1996, an exceptional Navidad year. The drogued buoy moved from the Celtic Sea near 50°N along the continental shelf margin west of Ireland and entered the northern North Sea, passing north of the Shetland Isles (61°N), between December 1995 and March 1996, passed through the LOIS/SES study site and reached speeds of 66 cm s^{-1} along the Malin shelfbreak (January 1996). Associated pulses of warm water progressing northward and entering the North Sea can be seen in the COADS distribution of sea surface temperature (January 1996). To the south, off Lisbon (Portugal; 38°N), temperature measurements at 212 m (from current meter mooring 147, 38°24.5′N, 09°30.3′W) showed values of 14.2°C in November–December 1995; in January 1994 (a weak Navidad year), the maximum temperature at the same depth (also mooring 147) was about 13.0°C.

[17] Overall, Figures 4, 5, and 6 and the related measurements show that in years of exceptional winter warming the ocean pool of Eastern North Atlantic Central Water (ENACW) has a warmer winter eastern boundary that will contribute to warmer and milder winters for European Shelf Seas.

3.1.4. NAO-SST correlations in the North Atlantic Eastern Boundary

[18] The relationship between N–D NAO and January sea surface temperature observed in the Cantabrian region (Navidad, see Figures 3c and 3d) was examined at additional shelfbreak/slope sites. Triangles in Figure 4 indicate these locations in the Eastern Boundary of the North Atlantic: the Iberian slopes (40°N 9°30′W), the Armorican slopes (46°N 4°W) and the Celtic Sea slope (48°30′N 10°W) near Goban Spur. The relationship was not analyzed at higher latitudes as January SST data was not available for most of the years. The results are presented in Figure 7 and extend in latitude the interannual climatic variation of January SST observed for Navidad (near 44°N; see Figures 3c and 3d). The correlations between N–D NAO and January SST of Figure 7 were also examined in the Iberian region (40°N) away from the influence of the continental slopes (at 15°W, 13°W and 11°W). The analysis showed much weaker correlations at 15°W ($r^2 = 0.2$), at 13°W ($r^2 = 0.3$) and at 11°W ($r^2 = 0.4$) showing that the relationship between N–D NAO and January SST was restricted to a region close to the continental slope margin, where the warm poleward flow is geostrophically constrained (see Figure 4). In the oceanic Bay of Biscay north of Navidad (45°N 5°W), the same association was tight ($r^2 = 0.95$), suggesting slope water shed to ocean from the Spanish and French slopes (see for example Figure 1c).

3.1.5. The 1996 Winter Swoddies in the SE Bay of Biscay

[19] Figure 7 also showed a larger regression slope, b, at 4°W (43°30′N b = 0.82 and 46°N b = 0.78) than at 10°–8°W (40°N b = 0.37 , 44°N b = 0.58 and 48°30′N b = 0.44). For the Navidad region (see dashed lines), the maximum SST difference from 8°W to 4°W was observed on January 1979 (~1°C), and the minimum (Navidad warm water near homogeneous from 8°W to 4°W) was observed in January 1990, 1996 and 1998 near where the regression lines cross (see also Figures 3c and 3d). We expected that these three years would produce more slope water eddies from the French and Spanish slopes. In the AVHRR archive (1979–2000), a pronounced production of swoddies in the SE corner of the Bay of Biscay was found in January 1990 (Figure 1c) and January 1996 (Figure 1b). *Pingree and Le Cann* [1992a] described the 1990 sequence and a sequence of the 1996 swoddy shedding is described below (Figure 8). During January 1998, a single swoddy, F98, was observed in the region (Figure 5b). We note however that during the 1994 weak Navidad year the AVHRR archive also showed the production of a single swoddy, F94, from Cap Ferret

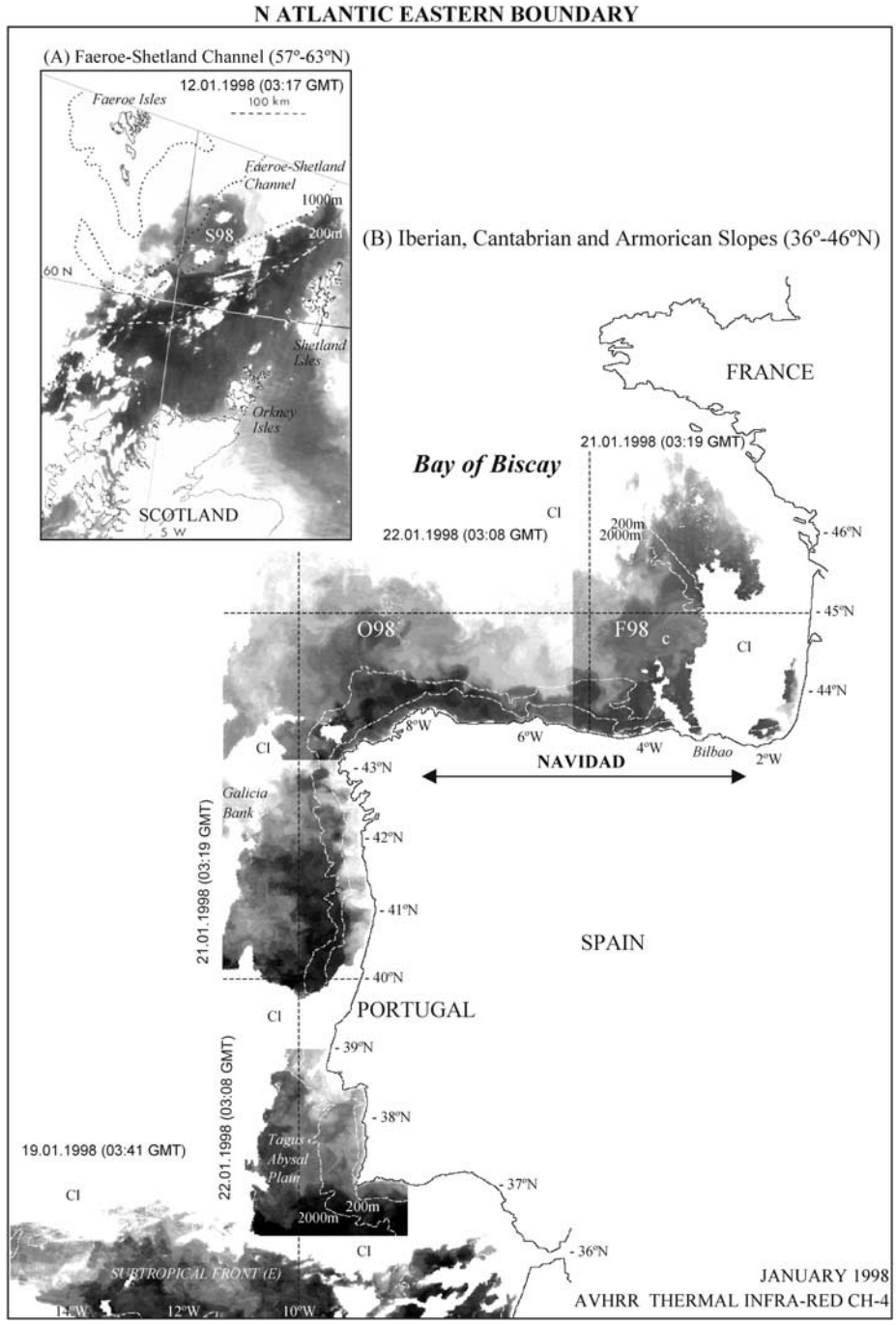

Figure 5. (a) AVHRR image for 12 January 1998 (0317 GMT) showing warm winter water along the West Shetland slope and shelf. The 200 m and 1000 m contours are shown. The West Shetland shelfbreak (200 m) is shown as a white dashed line. The warm (dark tone) slope water is bounded to the west by the 1000 m contour. Warm water of slope origin enters the Northern North Sea through the Fair Isle Channel between the Shetland Isles and the Orkney Islands. Some warm water leaves the slope and forms a swoddy-like (S98) structure in the deeper (1000–1500 m) Faeroe-Shetland Channel. (b) Composite AVHRR image for 19 (03:41 GMT), 21 (0319 GMT), and 22 (0308 GMT) January 1998 showing warm winter water along the Iberian, Cantabrian, and Armorican shelf/slopes. 200 m and 2000 m depth contours are shown (white dashed line). ''Cl'' denotes cloud. In the Bay of Biscay region, slope warm water is being shed to the ocean from near Cape Ortegal and Cape Ferret Canyon giving birth to swoddies O98 and F98. The ''c'' indicates an associated cyclone.

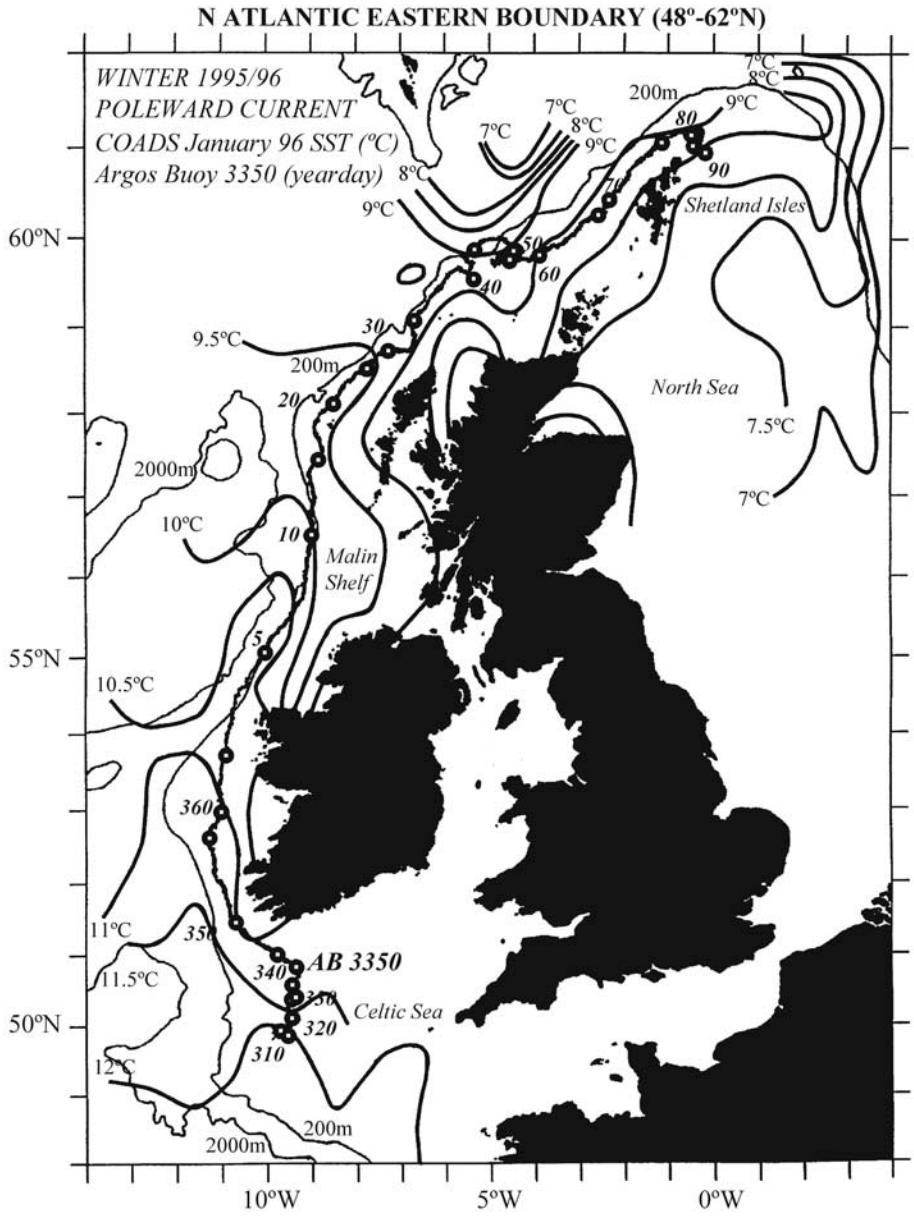

Figure 6. Distribution of COADS sea surface temperature (°C) during January 1996 showing pulses of warm water along the shelfbreak region from the southern Celtic Sea to the northern North Sea. The Lagrangian track of Argos buoy 3350 (drogued at 45 m depth) [from *Pingree et al.*, 1999b] showing simultaneous in situ measurement of poleward current has been included. A thick circle represents 5 days, and the buoy track shown extends from 8 November 1995 (yearday 308) to 31 March 1996 (yearday 90). Maximum buoy speeds occurred during early January 1996. The 200 m and 2000 m depth contours are shown.

Canyon [*Pingree*, 1994b], indicating that a weak Navidad is not opposite to the idea of the presence of poleward flow.

[20] During the winter 1995/1996 (Figure 8), an anticyclonic slope water eddy was observed by 5th and 8th January. We have referred to this swoddy as B96a as it developed from an offshoot of Navidad warm water near the slope constriction of Cap Breton Canyon. B96a showed a maximum development by 10 January, and by 17 and 18 January had evolved into a clear dipole structure. The cyclonic and anticyclonic components of this eddy pair were associated with smaller eddy substructures. The IR images on 17 and 18 January showed further swoddies in the process of being formed: a second swoddy B96b from Cap Breton, a swoddy F96 from near Cap Ferret Canyon, and a further instability R96 near 46°N (near La Rochelle Canyon). On 22 January, F96 was leaving the continental slopes and was associated with two cyclonic eddies. A tripole structure has also been described in the early stages of F90 [*Pingree and Le Cann*, 1992a] (see also Figure 1c). Further observations and tracking of these structures, including F96, was not possible due to the absence of cloud-free satellite images. Overall, swoddy production, as

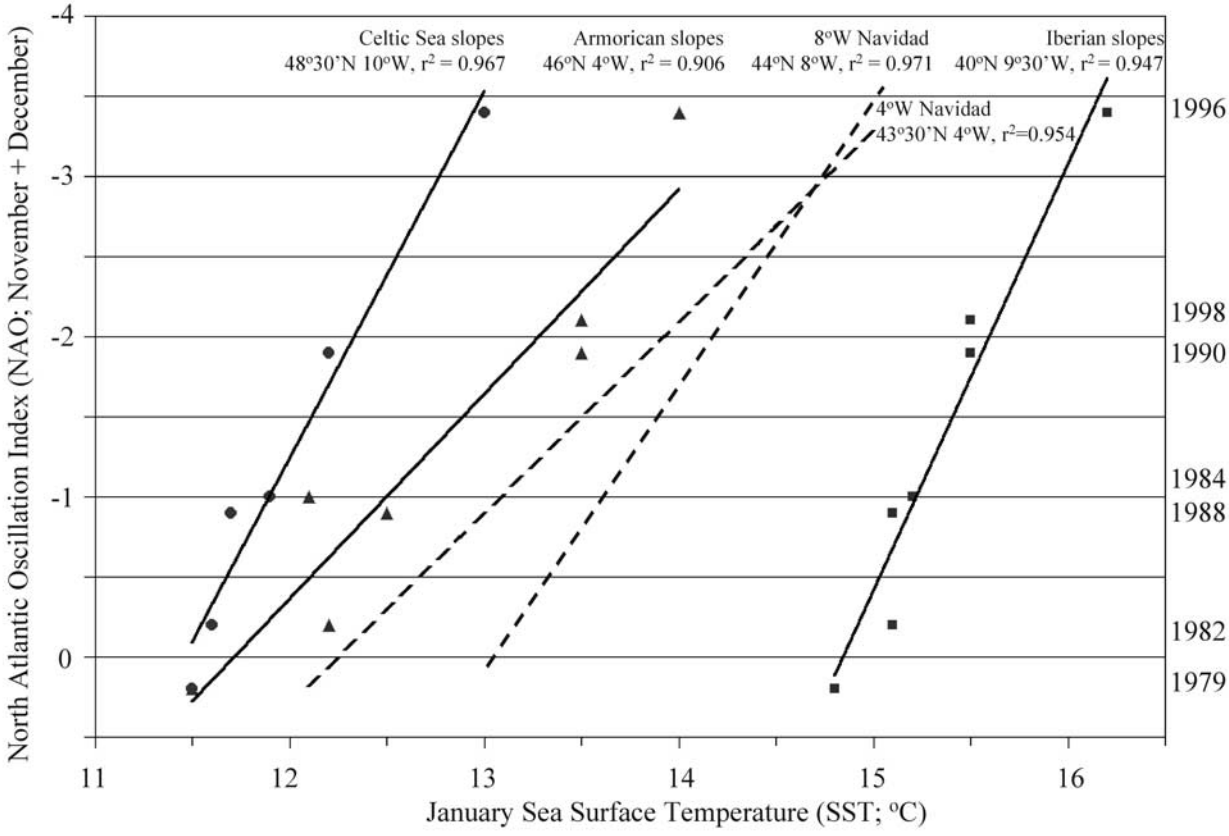

Figure 7. Relationships between the N–D NAO Index and January SSTs at the Iberian slopes (40°N 9°30′W), the Armorican slopes (46°N 4°W), and the Celtic Sea slope (48°30′N 10°W) during marked Navidad years. The number of observations is low (n = 7; n = 6 at the N Celtic Sea slopes) but the correlations are tight and significant (r^2 = 0.95 at 40°N, r^2 = 0.91 at 46°N, and r^2 = 0.97 at 48°30N). The Navidad correlations found at 4°W 43°30N and 8°W 44°N (from Figures 3c and 3d) are also included as broken lines (r^2 = 0.95 at 4°W and r^2 = 0.97 at 8°W). Shelfbreak/slope positions are shown (as triangles) in Figure 4.

in the 1996 example shown here, represents one way in which heat in the winter slope current is spread back into the adjacent ocean, and therefore can have a local climatic significance. These eddy structures have been observed in AVHRR imagery from Lisbon to Shetlands (Figure 5). A swoddy-like structure, SL92, was observed to leave the slope region off Lisbon in late December 1991 [see *Pingree and Le Cann*, 1993]. This eddy probably had a core of slope water from the Mediterranean Sea, making this eddy a smeddy or a meddy.

3.1.6. Twentieth Century SST Decadal Trends in the Navidad Region and Celtic Shelf (1890–2000)

[21] The winter poleward flow of warm water represents a significant winter climate change for the slope region as warm water is collected from the ocean and transferred northward along the slopes. The continental slope region in turn warms the adjacent ocean and shelf region as warm winter water is injected into the ocean, in some cases by the production of swoddies or transferred across and on shelf by Ekman transport or wind driven surface currents for example. We have analysed here (see Figure 3b) a long-term time series (1967–2000) of SST in the Cantabrian shelf/slopes in relation to marked AVHRR occurrences of Navidad (1979, 1982, 1984, 1988, 1990, 1996, and 1998). This temperature time series includes other warming and cooling cycles of lower frequency. The results show that mean sea surface temperature in the Navidad region has a maximum ~20y change from a minimum value of 12°C near year 1976 to a maximum temperature in 1996 of 15°C (Figure 9a). A temperature increase of ~1.4°C is observed for the same period after applying a 5y running mean (Figure 9c; dashed line).

[22] We can extend these SST observations in a secular timescale by comparing them with the long-term trend (1890–1999) of annual SST values at the Celtic Sea (near 50°N 6°W; Figures 9b and 9c). Other relevant time series of SST derived in the North Atlantic include, for example, *Hagen and Schmager* [1991] from 1957 to 1974, *Loeng et al.* [1992] from 1921 to 1990, and *Levitus et al.* [2000] from 1948 to 1998. Long-term time series of air temperature in the NE Atlantic are shown for example by *Alheit and Hagen* [1997] (1659–1963 data; see also *Manley* [1974]) and by *Lavín and Cabanas* [2001] (1960–2000 data from INM). *Mann et al.* [1999] show northern hemisphere surface temperatures using multiproxy data over the last 1000 years. In the adjacent Navidad and Celtic Sea regions analyzed here, SST time series over long periods will not diverge and so we observe a significant correlation (r^2 = 0.71) of the 5 y

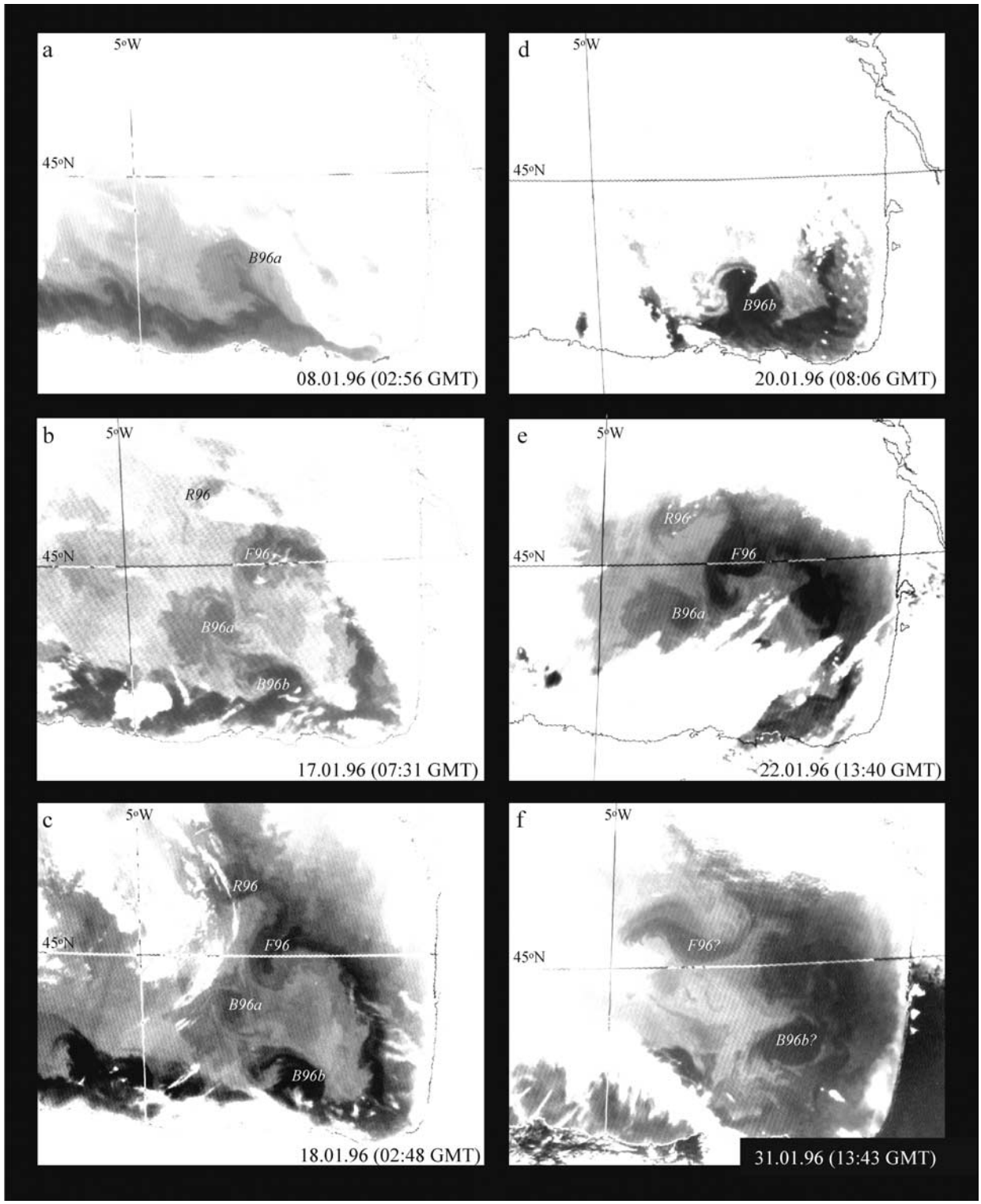

Figure 8. A selection of IR satellite images showing warm water structures leaving the continental slope in the SE corner of the Bay of Biscay in January 1996. (a) The 08.01.96 image showing initial stages of development of B96a from the slope constriction associated with the southern side of Cap Breton Canyon. (b) The 17.01.96 image showing second swoddy B96b developing from the vicinity of Cap Breton and F96 forming from slope water shed near Cap Ferret Canyon. A further instability is apparent near 46°N. (c) The 18.01.96 image with eddies labeled. (d) The 20.01.96 image showing position of B96b. (e) The 22.01.96 image showing relative positions of warm water (swoddies) leaving the continental slope. (f) The 31.01.96 image with warm water feature probably B96b on Landes Plateau and further detachment of feature that appears to be a development of F96. Thermal contrast (AVHRR SST) is about 2°C between warm Navidad waters (~15°C) and cooler adjacent ocean waters (~13°C).

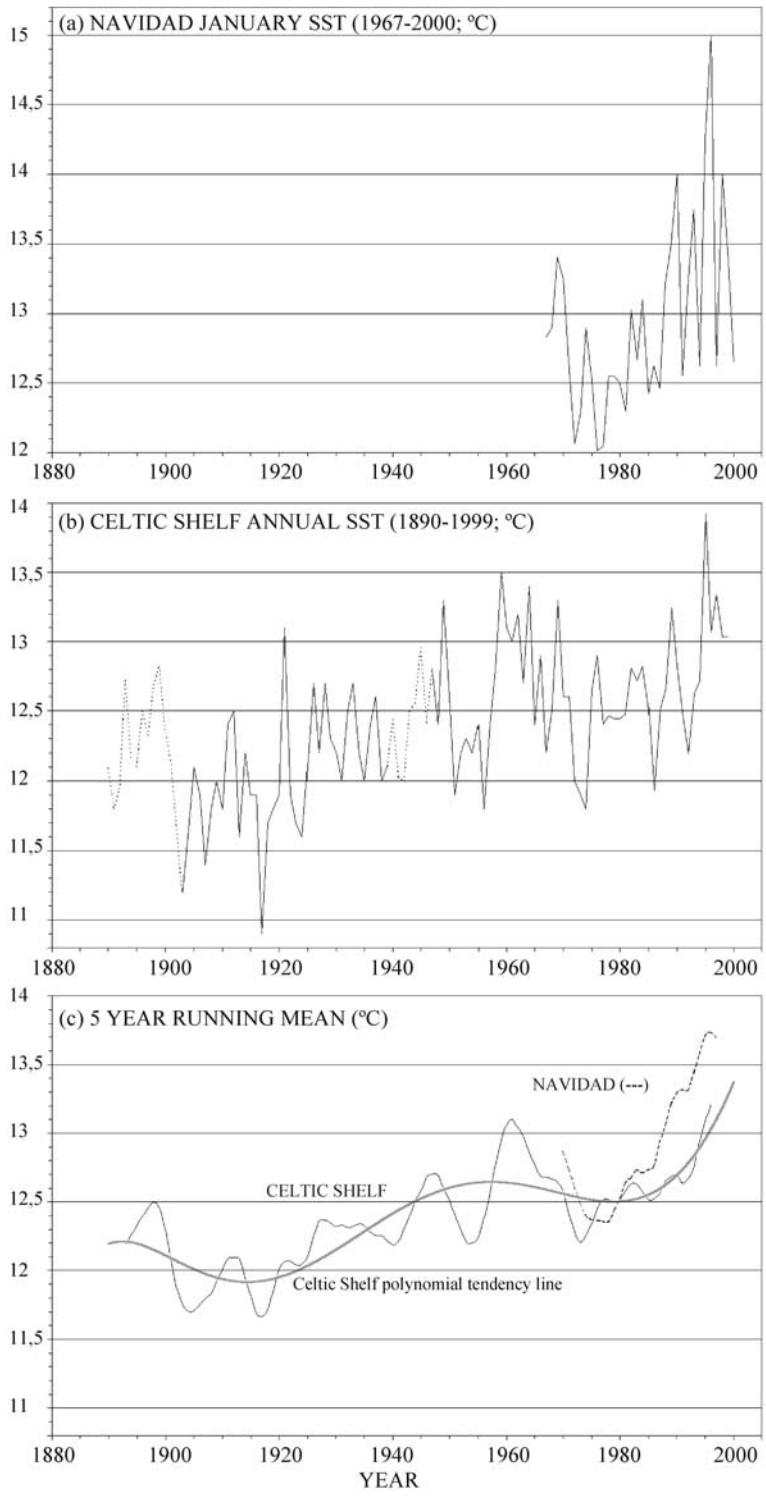

Figure 9. (a) January sea surface temperature (SST) in the Navidad region for years 1967–2000. The plotted values represent the average of monthly January SSTs at 4°W and 8°W along the Cantabrian shelf/slopes (see Figure 3b). (b) Annual sea surface temperature at Seven Stones (Celtic shelf; near 50°N 6°W) for the 20th century (1890–1999; see text for details). Dotted values interpolated from other local data. (c) 5 y running mean of the Navidad (dashed line) and Celtic Shelf (continuous line) SST time series. A polynomial tendency line (order 6) accounting for 38% of the variance of the annual Celtic shelf data (frame b) is also shown. The positions of the SST measurements (4°W and 8°W Navidad regions and Seven Stones) are shown in Figure 4.

running mean data for the overlapping years (1967–1999; see Figure 9c). The long-term trends in the Navidad region are derived from January SST values but will be fairly representative of the trends derived from annual values. Long-term warming trends in the Bay of Biscay for the period 1972–1993 [*Koutsikopoulos et al.*, 1998] have been derived from summer (July–September) and winter (January–March) data showing comparable results. The long period trends in the Navidad region are also not local as the sea regions to the north and south are not isolated (see Figure 4, for example) and experience similar climate heating influences.

[23] Overall, from combining the Navidad and Celtic shelf long-term observations (Figure 9c) we could say that over the last century there has been a fall of temperature of about 0.3°C from ~1890 to ~1915. Sea surface temperature increased about 0.7°C from ~1915 to ~1960. A maximum temperature occurred near 1960. From ~1960 to ~1980, there has been an small fall of about 0.1°C. This has been followed by a rise of about 0.8°C to ~1998. The net effect of these decadal changes of SST is an increment of the sea surface temperature of ~1°C over ~100 years. In the Navidad and Celtic shelf observations there are also periodicities of 10 years and less with perhaps a suggestion of a longer ~20 year periodicity with increasing amplitude from past to present. Inevitably, there is always more interest in the latest trend which is associated with the maximum amplitude anomaly. At present, only further observations will show whether the increasing temperature trend, very evident near the end of the 20th century, will continue into the 21st century or whether it is just part of a longer period fluctuation.

3.1.7. Winter Warming Heat Flux Along the European Continental Slope/Shelf Margin

[24] We have measured and collected sufficient data in the previous sections to appraise the importance of the slope current in the annual heat budget for the NE Atlantic continental shelf margin. We estimate now the heat flux provided by the January slope current at some mean position between 40°N and 60°N for a year of exceptional warming, assuming steady state conditions for the month. January poleward currents of say 10 cm s^{-1} would result in displacement of slope water of about 300 km in a month. We note that buoy 3350 travelled 1600 km along the shelfbreak in 137 days (4.5 months). The temperature drop along the slope is about 1°C per 500 km. If we assume that the current (10 cm s^{-1}) is representative of the upper 100 m of the water column (which in January is generally well-mixed), then this advective heat flux is equivalent to a heating of $\sim 5 \times 10^3$ cal cm^{-2} $month^{-1}$ through unit area of the sea surface in a streamline set in the slope margin. This heating is equivalent to about an extra month of summer net heating for the slope region at a rate equivalent to the mean of the summer months (mid March to mid September) of the annual net heating cycle for the Armorican and Celtic Sea regions [*Pingree*, 1975]. If we assume the 'slope heat conductor' to be about 30 km wide (i.e. the width over which the along slope current of 10 cm s^1 might apply) then this heat flux is applied to a region about 10^5 km^2. It is important to realise that this additional regional net advective heat flux for the continental slope does not come from the subtropics but is collected at all latitudes where the winter poleward transport increases with latitude. The value for the extra heat flux given is also likely to be an underestimate (for a marked Navidad year) as poleward flow in December and February would increase the period over which the slope heat conductor operates effectively.

3.2. Remote Sensing and Seatruth Measurements of Summer Swoddies

[25] The first Part of this study has examined the production of winter swoddies through different aspects of Navidad and poleward warming and the leakage of poleward warm water associated to abrupt changes of shelf/slopes width and orientation. This second part of the study focuses on the structure of swoddies (F90) or swoddy-like eddies in the southern Bay of Biscay during summer following two years of exceptional Navidad (1990 and 1998). We analyse recent remote sensing data (simultaneous IR, altimeter and SeaWiFS data) and seatruth measurements (SeaSoar and ADCP measurements) with an aim to understanding the chlorophyll *a* distribution from the described satellite-observed and in situ physical structure.

3.2.1. Long-Term AVHRR Observations of Anticyclonic Eddies (1979–2000) and Swoddy Core Temperatures

[26] We have identified the central position of the summer swoddy-like eddies in the AVHRR archive (1979–2000) by using the characteristic sea surface cooling signature of swoddy F90 near its centre due to doming of the seasonal thermocline [*Pingree and Le Cann*, 1992a] (see, for example, Figure 2). The individual observations for different years are shown in Figure 10 and a summary of the central location of all eddies is presented in Figure 11. Table 1b lists some characteristics of the satellite images used.

[27] The analysis by years (Figure 10) indicates that the summer swoddy-like eddies in the region can be found when the Navidad expression (late December–January) has been marked (1979, 1982, 1984, 1988, 1990, 1996, and 1998 eddies) or weak (1986, 1991, 1992, 1993, 1994, and 1995 eddies) but also in years without a clear Navidad development along the Cantabrian shelf (1983, 1987, 1999, and 2000 eddies). However, the observations at 4°W (4°W eddies) [*Pingree and Le Cann*, 1992a] appear confined to years of marked Navidad (4°W eddies during 1979, 1982, 1990, and 1996) and the observations during years without a clear Navidad structure (see white circles in the pluriannual summary of Figure 11) tend to be distributed to the west of ~6°–5°W, perhaps indicating swoddy production only near the N Iberian promontory (e.g., eddies shed from near Cape Ortegal). The distribution can also reflect a generally westward movement of anticyclonic eddies if they are generated near the French and N Spanish slopes. Overall, the southern envelope of centres is about 50 km from the Spanish continental slopes (~1000 m depth contour) so the azimuthal velocity of the eddy could be experienced in the upper slope region and would be registered in current meter observations (with swoddies reversing any poleward flow). Topographic β effects do not allow an eddy core to cross the continental slope and so swoddies or eddy-like structures do not occur on the continental shelf (in a wide shelf context, e.g., Celtic Sea).

[28] Figure 11 also shows in annotations the summer eddies that have been surveyed at sea: swoddy F90 (1990)

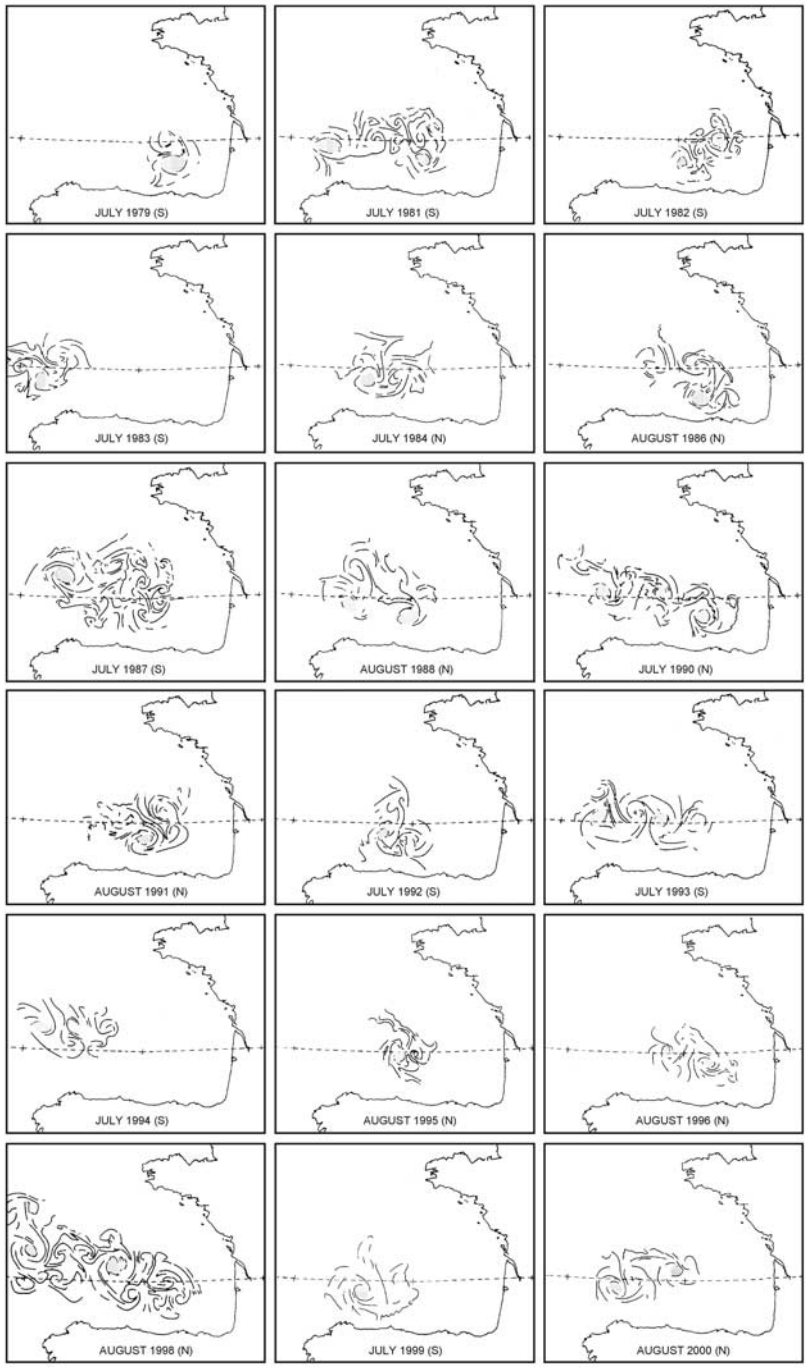

Figure 10. Observations of swoddy-like anticyclonic eddies in the southern Bay of Biscay (south of 46°N) during summer (July or August) for the period 1979–2000. The drawings have been elaborated from regions of thermal contrast in enhanced AVHRR thermal infrared (channel 4) images. Shaded regions in the frames highlight the center of the swoddy-like anticyclonic eddies that show a cool surface signature due to doming of the seasonal thermocline (see, for example, Figure 2a). N and S annotations indicate a northbound (N) or southbound (S) satellite projection of Dundee Satellite Receiving Station (DSRS). Other characteristics of the satellite images are listed in Table 1b.

and swoddy-like eddies × 91 (1991), AB3917 (1992), and AE6 (1998). The temperature measurements in the core (at 150 m depth) of these eddies might suggest a relationship between core temperature and strength of the previous Navidad. Values of ∼12.95°C (CTD) and ∼12.60°C (CTD) were observed during years of marked Navidad (data from *Discovery* 193 cruise data in July 90 and data from *Professor Shtokman* cruise 8/98 in August 1998). Values of ∼11.75°C (XBT) and ∼11.688°C (CTD) were recorded during years with a weak Navidad (data from BSHM *Ailette* cruise in September 1991 and data from *Charles Darwin* cruise 66 in April 1992). Temperatures at

Table 1b. Summary of Characteristics of AVHRR Satellite Images (Enhanced Channel 4) From Dundee University Used for Long-Term (1979-2000) Observations of Summer Swoddy-Like Eddies (Figures 10 and 11)[a]

Date	Time	NOAA	Orbit	DSRS ID	Published Images and Cruise Investigations
25.07.79	1356	T-N	4021	218/08B	
25.07.80					no clear structures (ncs)
28.07.81	1405	N-7	496	308/04B	two anticyclonic eddies in August 1981 [*Pingree*, 1984]
10.07.82	1342	N-7	5390	388/10A	
05.07.83	1503	N-7	10477	406/13A	
18.07.84	0820	N-6	26227	469/08A	
18.07.85					ncs
06.08.86	0407	N-9	8487	609/04A	
04.07.87	1453	N-9	13177	675/12A	
06.08.88	0802	N-10	9791	753/12A	
06.08.89					ncs
11.07.90	0805	N-10	19804	888/09B	Swoddies F90 and 4°W in July 1990 [*Pingree and Le Cann*, 1992a] *Discovery* cruise 193 (July 1990)
11.07.90	1328	N-11	9240	888/10B	Figure 2a showing swoddy F90
02.08.91	0254	N-11	9544	892/09A	Figure 2b showing swoddy F90
04.08.91	0302	N-11	14723	1058/03	anticyclonic eddy X91 in July 1991 [*Pingree and Le Cann*, 1994a] BSHM *Ailette* 9/91 cruise (September 1991)
02.07.92	1437	N-11	19431	1184/08	an anticyclonic eddy in July 1992 [*Pingree*, 1994a] *Charles Darwin* cruise 66 (April 1992)
06.07.93	1542	N-11	24642	1323/11	
14.07.94	1645	N-11	29910	1464/01	
17.08.95	0801	N-12	22112	1611/12	
17.08.96	0259	N-14	8404	1795/11	
17.08.97					ncs
07.08.98	0653	N-12	37553	2223/13	anticyclonic eddies AE6, BE10, and CE12 in August 1998 *Professor Shtokman* cruise 898 (August 1998) Figure 12 showing simultaneous AVHRR, altimeter (combined TOPEX/Poseidon/ERS-2 data), and SeaWiFS measurements
08.07.99	1458	N-14	23297	2417/08	
09.08.00	0551	N-12	47978	2468/11	

[a] The 1979–2000 most clear observations of summer (July/August) swoddy-like eddies (Figures 10 and 11).

the eddy core in these in situ observations are about 1°C cooler than the 4°W January SST. With the exception of swoddy F90, it is not possible to estimate when or where these summer swoddy-like eddies were formed and so further relevant measurements are required to establish a more formal relationship between core and Navidad temperature. However, intensive summer studies were conducted for AE6 (1998) and F90 (1990) using both remote sensing data and seatruth measurements.

3.2.2. AVHRR, Altimeter, and SeaWiFS Satellite Data of 1998 Swoddy-Like Structures

[29] The remote sensing signature of swoddy-like eddies was investigated during summer 1998 using additional color and altimetric sensors (i.e., SeaWiFS and TOPEX/ERS-2). Simultaneous observations of sea surface temperature (AVHRR sensor; 7 August 1998), chlorophyll *a* concentration (SeaWiFS sensor; 7 August 1998) and Sea Level Anomaly, SLA, (combined TOPEX/Poseidon/ERS-2 data; 2–11 August 1998) were made. The results, presented in Figure 12, correspond to the *Professor Shtokman* cruise period in August 1998 (see cruise data by Fernández et al. (submitted reference, 2002)). For these observations, it was not possible to have a sequence of AVHRR observations that could link clearly the anticyclonic eddies to a slope water origin but we note that 1997/1998 was a year of exceptionally marked winter warming and exhibited production of at least two swoddies (F98 and O98; see Figure 5b). Observations from the AVHRR sensor (Figure 12a) show the presence of three anticyclonic swoddy-like structures (labeled AE6, BE10 and CE12) in the Southern Bay of Biscay centred near longitudes 6°W (45.5°N 6°W), 10°W (45.75°N 9.75°W) and 12°W (45.5°N 11.5°W) based on centre of surface cool signatures. The altimeter data (Figure 12b), with lower resolution, showed the same anticyclonic structures as maximum SLA of ~ +10 cm with a diameter of ~100 km. The observed values of SLA were comparable to the dynamic height anomaly (8 cm) derived from field data (CTDs; F90). In the SeaWiFS chlorophyll *a* image (Figure 12c), the signature of the three eddies results from chlorophyll *a* rich filaments (up to 1.0 mg Chl *a*/m^3) circulating in a clockwise sense around the N, E and S eddy margins. The chlorophyll *a* content of these filaments increases toward the northwest where chlorophyll *a* level are generally higher since here the productive season is delayed. The chlorophyll filaments are matched with cooler water structures from the north (~46.5°N) in the AVHRR image. In like manner, the dynamic structure associated with the SLA gradient draws warmer chlorophyll *a* poor surface water from the south around the western flank of each eddy. Advection of phytoplankton, as the examples shown here for summer anticyclonic eddies, has also been reported for the Armorican and Celtic slope current [*Garcia-Soto and Pingree*, 1998] and for a coastal wind-induced current in the Western English Channel [*Garcia-Soto et al.*, 1995]. Observations from the three sensors also show that the swoddy-like structure at 6°W (AE6) is associated with two smaller cyclones, where the sea surface is depressed by about 2 cm, with centers to the SE and NNW at a radial

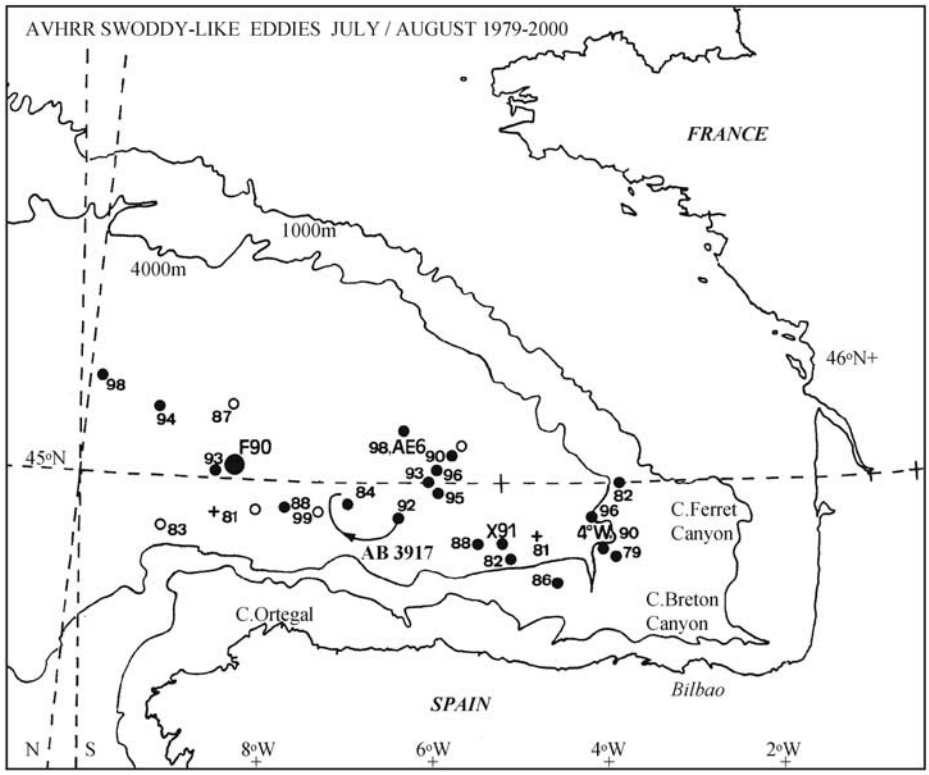

Figure 11. Summary of the central locations of summer swoddy-like eddies in the southern Bay of Biscay (south of 46°N) for the period 1979–2000. The individual observations of the eddy structures are shown in Figure 10. The 1000 m and 4000 m depth countours are shown. Black dots indicate observations during years of marked and weak Navidad. Observations during years without Navidad structure are shown with white circles; an unlabeled white circle indicates year 2000 (00). The cross indicate a 1981 summer eddy without a previous Navidad observation due to cloud cover. AB3917 shows the July–August track of Argos buoy 3917 drogued at a depth of 320 m in the July 1992 swoddy-like structure [*Pingree*, 1994a]. AB3917 was almost certainly a swoddy F92 and probably formed in March shortly before the eddy survey in April 1992 [*Pingree*, 1994a]. Swoddy F90 (1990; see also Figure 2a) and swoddy-like eddies AE6 (1998; see also Figure 12), × 91 (1991) and AB3917 (1992) were measured at sea (see Table 1b) following winters of marked (1990 and 1998) and weak Navidad (1991 and 1992) respectively.

distance of ~110 km from the anticyclone center. Smaller cyclones are also associated with the other swoddy-like eddies (BE10 and CE12). The cyclones are also chlorophyll poor regions in summer. The coldest water in Figure 12a occurs in the upwelling region off NW Spain. The importance of an inorganic nutrient supply for a marked summer production is demonstrated by the high chlorophyll *a* content for this region (Figure 12c).

3.2.3. Seasonality of SeaWiFS Chlorophyll *a* Concentration at 45.5°N 6°W

[30] In order to put the SeaWiFS chlorophyll a results in an overall seasonal context we have analysed a time series of SeaWiFS chlorophyll *a* concentration (from September 1997 to April 2001) for the position of swoddy-like eddy AE6, which represents a fairly central position in the oceanic Bay of Biscay at 45°/46°N. Results presented in Figure 13 show that the summer SeaWiFS chlorophyll *a* concentration measured for August 1998 (representing conditions at the centre of the eddy) does not differ significantly from the value observed during August 1999 and August 2000. Summer levels are low (~0.2 mg Chl*a* m^{-3}) but not as low as summer values (~0.1 mg Chl*a* m^{-3}) to the south (34°N) [*Pingree et al.*, 1999a]. So it appears that during July/August the oceanic eddies mainly wind or redistribute the surface values (see Figure 12). In the productive season though the eddies may also play a role in local production [*Garcia-Soto and Pingree*, 1998] they are also observed to influence the Spring bloom zonal pattern as it migrates northward (Figure 14). The Spring Bloom occurs in March/April somewhat earlier than at 47°N (April/May) [*Garcia-Soto and Pingree*, 1998]. In the seasonal results (see Figure 13), we note that the 1998 Spring Bloom response appears considerable smaller than the 1999 one. A longer time series would be required to state whether there is any relationship between the occurrence of a marked Navidad and the intensity of the following Spring Bloom.

3.2.4. Biological Response to Swoddy F90 Thermocline Structure (*Discovery* 193 cruise; July 1990)

[31] During the 22 years of IR observations (1979–2000), swoddy F90 is so far the only swoddy that has been hydrographically surveyed (July) [*Pingree and Le Cann*, 1992a] and then subsequently tracked back with AVHRR to its birth off Cap Ferret canyon (January). Thus, this swoddy represents a standard against which measurements of swoddy-

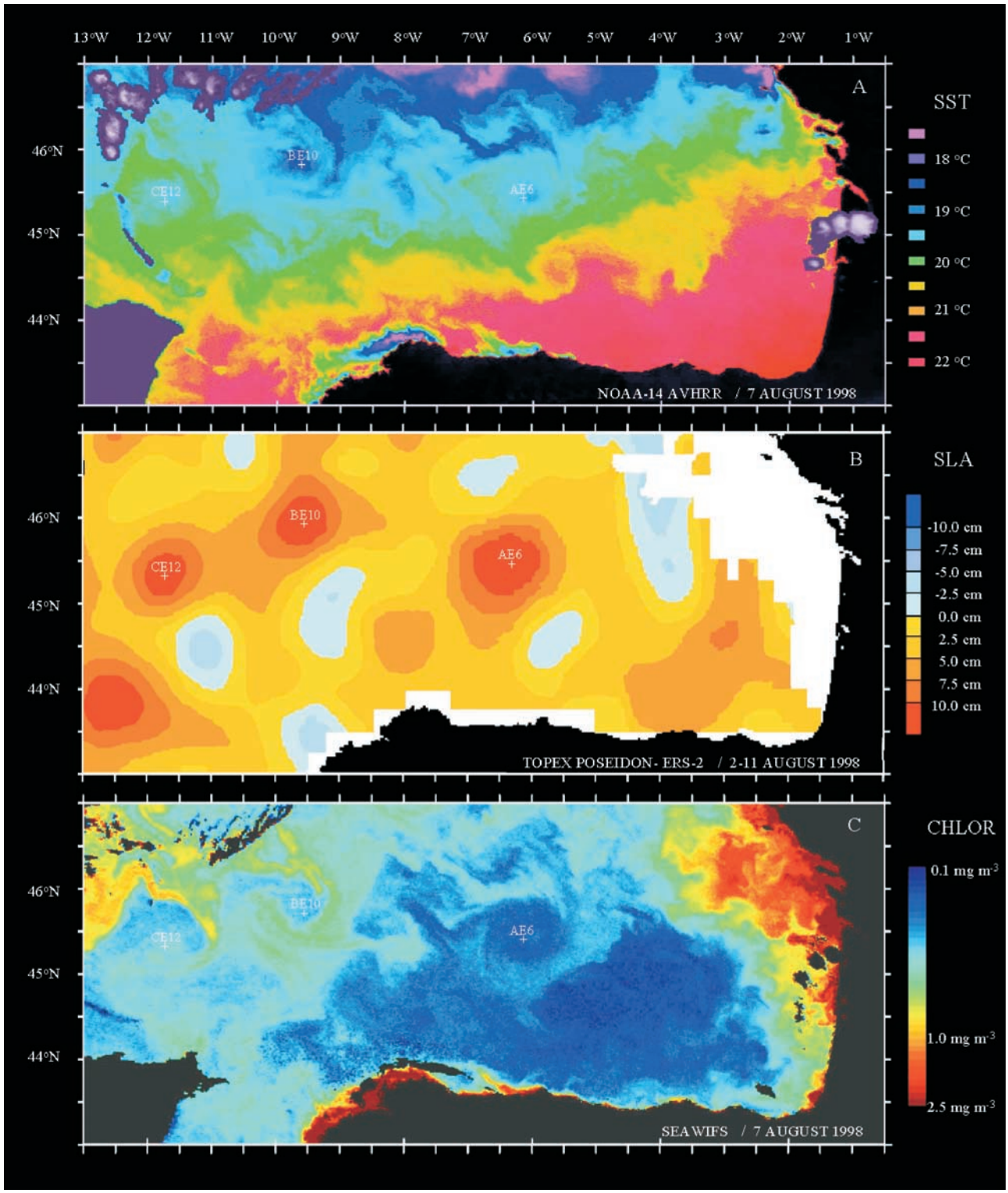

Figure 12. Simultaneous remote sensing observations of summer swoddy-like eddies following a marked winter Navidad (1998) from three different satellite sensors showing swoddy-like signatures in (a) AVHRR (sea surface temperature (SST); 7 August 1998), (b) combined TOPEX/Poseidon/ERS-2 altimeter (sea level anomaly (SLA); 2–11 August 1998), and (c) SeaWiFS (chlorophyll *a* concentration; 7 August 1998) data.

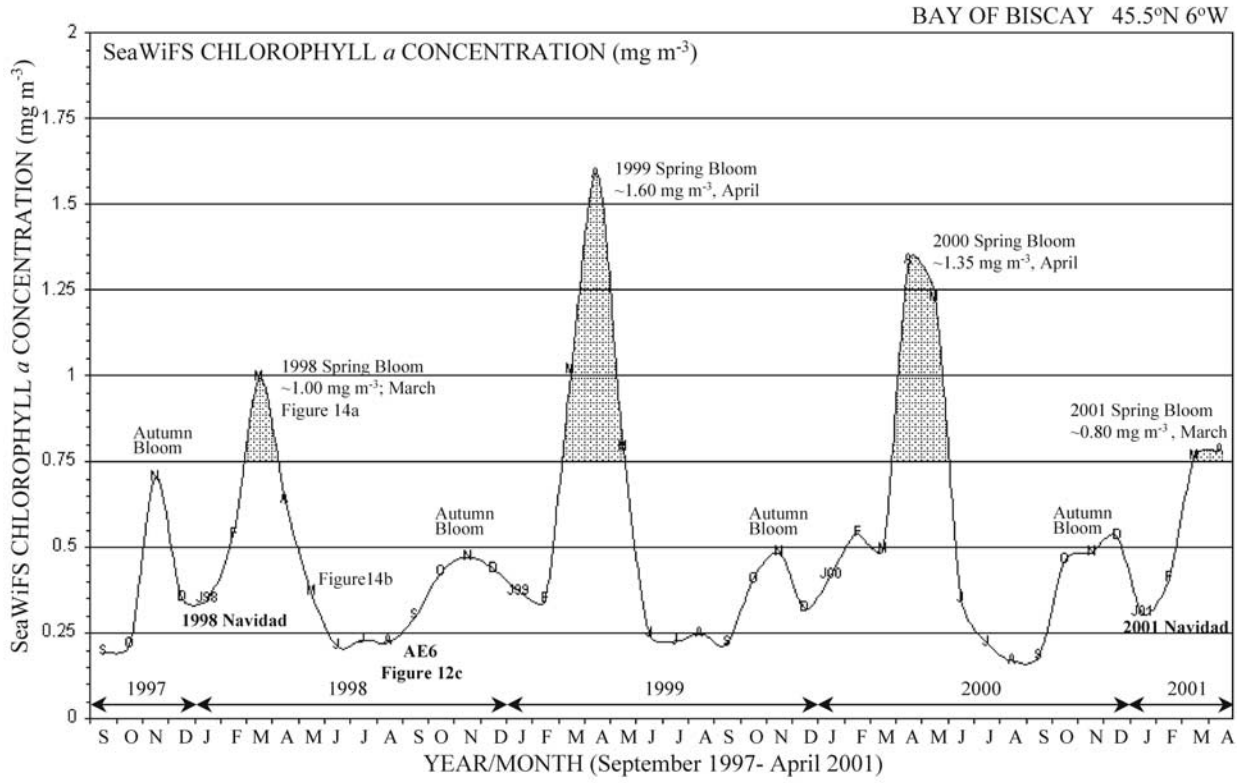

Figure 13. Time series of monthly SeaWiFS chlorophyll *a* concentration (mg Chl*a* m^{-3}) in the Bay of Biscay (45.5°N 6°W) from September 1997 to April 2001. Each value represents the average of 24 pixels around a central position. The position chosen is near the center of swoddy-like eddy AE6 in August 1998 (see Figure 12c), which is seen to have a normal minimum summer value (~0.2 mg Chl*a* m^{-3}).

like eddies can be compared. *Pingree and Le Cann* [1992a] gave the overall eddy structure and properties. Here we use some of the same *Discovery* 193 cruise data to illustrate the small-scale spatial structure associated with F90. This will be important in determining the levels of chlorophyll *a*. Figure 15 presents SeaSoar chlorophyll *a* relative fluorescence levels (mg Chl*a* m^{-3}) and Brunt-Vaisala frequency (cph) from sections through the swoddy (see Figure 2d). SeaSoar temperature perturbation profiles through F90 (Figure 16) and ADCP current structure (Figure 17) are illustrated from the survey shown in Figure 2c.

[32] Temperature sections (Figure 15b) show the stability of F90 in relation to the external conditions representing the Bay of Biscay. The Brunt-Vaisala frequency (Figure 15c) has been derived over a vertical interval of 8 m and shows typical values in the eddy core of about <1 cph. The 0.5 cph contour has a corresponding period value of 2 h; in the centre of the core, a period of about 5 h was derived by *Pingree and Le Cann* [1992a]. Summer thermocline values are typically 10 cph. Chlorophyll *a* fluorescence (Figure 15a) peaks in the thermocline with increases over the eddy core where the thermocline is domed upwards (Figure 15b); these same fluorescence levels however can also be found at some exterior positions. At the sea surface, the cool region associated with the doming of the seasonal thermocline, has marginally increased surface fluorescence levels that decreases from the first (14 July; see Figure 16b) to the second survey (28/29 July; see Figure 15a), so in July a swoddy could show a marginal increase in SeaWiFS chlorophyll *a* levels associated with the eddy center. This increase might reflect vertical mixing or increased production in a more favorable nutrient and light regime. These surface chlorophyll *a* fluorescence signals cannot be compared directly with remote sensing data as the 1990 SeaSoar measurements fell in the gap between CZCS data (1978–1986) and SeaWiFS data (1997 operational). We note however that in August a central surface increase of chlorophyll *a* was not found in the SeaWiFS measurements (see Figure 12c) and in the cruise measurements (Fernández et al., submitted reference, 2002) of the 1998 swoddy-like eddies which only showed significant surface increases associated with the circulating filaments drawn from the north.

3.2.5. Cyclonic Eddies Associated with Swoddy F90

[33] In the earlier paper of F90 [*Pingree and Le Cann*, 1992a], the properties of the cyclones associated with the anticyclonic swoddy were not given. Here we briefly summarize the measured structure for cyclones and show that this results in contrasting fluorescence levels in the seasonal thermocline for cyclones with respect to the anticyclone. In Figures 2a and 2b, there are two to three smaller (~50 km diameter) cyclones associated with the exterior region of the anticyclonic swoddy F90. The anticyclone is typically about 50% larger than a cyclone and the distance between the anticyclone and cyclone centers is about 100 km. Both structures appear to penetrate to a depth of about 1km. The most conspicuous cyclone to the east, with the centre near

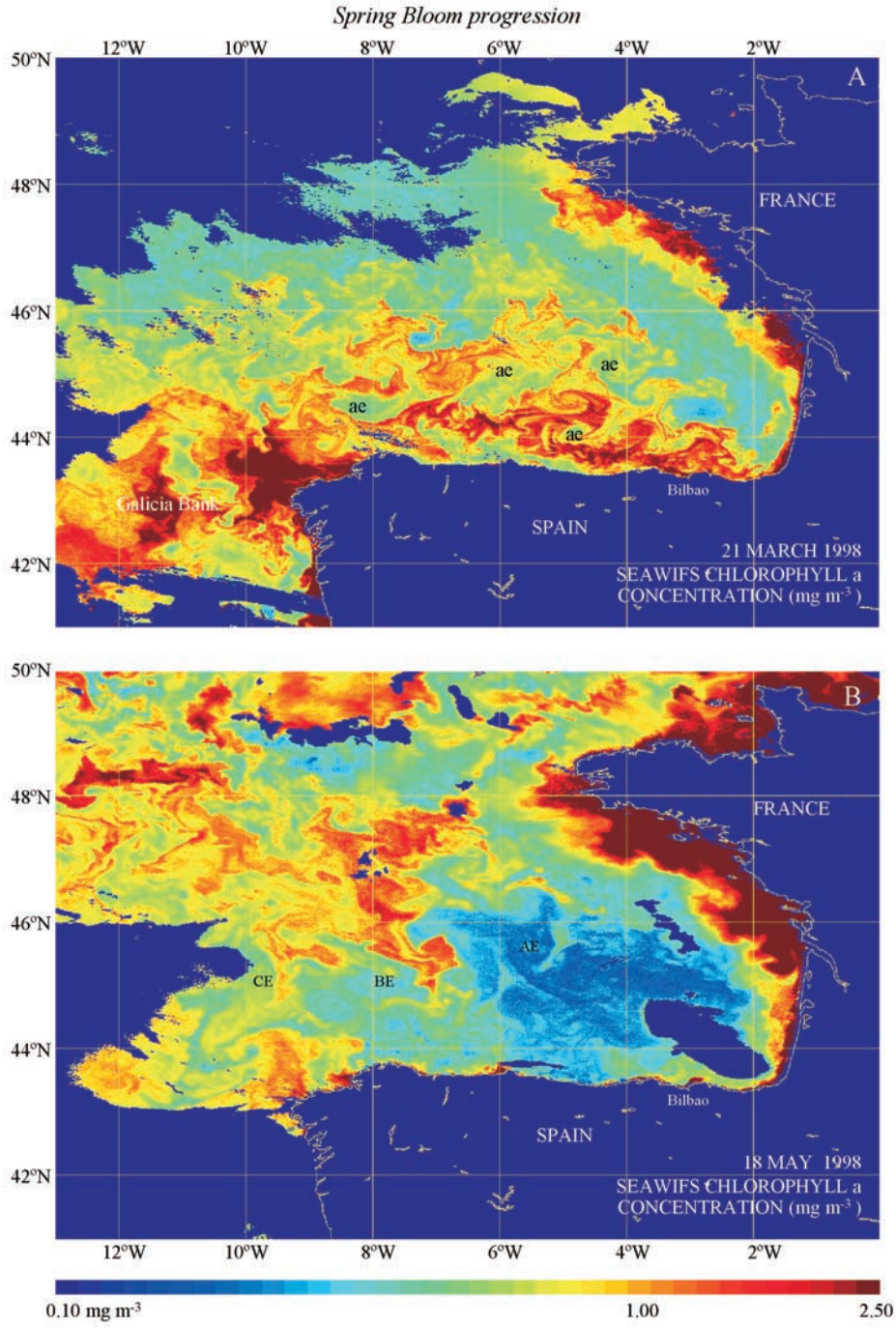

Figure 14. SeaWiFS satellite images of chlorophyll *a* concentration for (a) 21 March 1998 and (b) 18 May 1998 showing development and northward progression of the Spring Bloom of phytoplankton in the Bay of Biscay and adjacent regions. During March, the highest phytoplankton concentrations (redish color) are located south of 46°N. Particularly high concentration of phytoplankton in March occurred over Galicia Bank and off the NW Spain upwelling region. During May, the Spring Bloom has progressed northward north of 46°N. Bloom development has occurred in the French shelf, Ushant Front and English Channel regions. Some anticyclonic eddies (ae) annotated in Figure 14a.

45°N 7°W, is evident in the SeaSoar section (Figure 15b). This cyclone has an absence of 13°C water (swoddy core water) at about 75 m, and below this depth the isotherms (isopycnals) are raised by about 100 m (due to squeezing of the isotherm thicknesses between 12°C and 13°C). This result is similar to other dipole structures where the water properties of the anticyclonic core corresponds to the absent water properties in the cyclone. This is believed to result in

the formation process where the anticyclonic core feeds isopycnically on the exterior regions surrounding the anticyclone. Vertical mixing tends to make the anticyclone center about 0.02 psu fresher than exterior regions and the cyclone center about 0.02 psu more saline on an isopycnal surface near the base of the core and these salinity anomalies may extend to the sea surface. The thermocline is raised in the anticyclone where the isopycnals are stretched and lowered or domed downwards in the cyclone where the isopycnals are squeezed. This results in the sea surface being about 0.5°C colder over the swoddy center and about 0.5° warmer over the cyclone center with respect to exterior regions. This temperature contrast associated with eddies of opposite sign can be seen in AVHRR images. The two low sea level anomalies indicating cyclones associated with the positive sea level anomaly of anticyclone, AE6, are warmer than the surface water in the center of AE6 (cf. Figures 12a and 12b). The 1998 August SeaWiFS structures also show that the cyclones or low SLA regions also have low levels of surface chlorophyll *a* (see Figure 12c). The most marked fluorescence difference between cyclones and anticyclone occurs subsurface in the seasonal thermocline where chlorophyll *a* levels in the anticyclone are almost double those of the cyclone. Over the swoddy core, the subsurface chlorophyll *a* maximum is at a depth of about 40 m whereas it lies about 20 m deeper (at about 60 m depth) near the cyclone center where the thermocline is most depressed (see Figures 15a and 15b). Hence, we do not expect a summer SeaWiFS surface signature for cyclones though anticyclones could show in early summer (July) an increase in fluorescence level at the sea surface near their centers (see Figure 16b). This contrast to the case at the start of the productive season where the cyclones have higher surface levels than anticyclones (Figure 14a). This results from the fact that before the thermocline is established cyclones have stability nearer the sea surface and anticyclones have a warmer, deeper mixed layer depth.

[34] At the edge of the anticyclone core the maximum azimuthal current are typically 30 cm s^{-1} whereas currents of 10–15 cm s^{-1} were measured to a depth of 400 m (ADCP) in the cyclone (labeled C, Figure 15) at a radius of ~25 km. The currents from cyclone and anticyclone may sometimes superpose resulting in jet-like structures between eddy centers where currents of 40 cm s^{-1} were measured (ADCP). Argos buoy 3919 [see *Pingree*, 1993], drogued at 300 m depth, made 2 loops in the cyclone at a radius of ~26 km with mean speed of 11 cm s^{-1} during the same period that Argos buoys 3909, 3918, and 5030 were moving anticyclonically around the swoddy center. From the buoy tracks, the distance between eddy centers was determined as ~105 km. Maximum speeds measured over a 24 h period were 25 cm s^{-1} and occurred when buoy 3919 was between the eddy centers near the jet region. The buoy track showed that the cyclones move anticyclonically around the swoddy and cyclone 'C' took about 1 month to complete ~45° of clockwise rotation. Anticyclone-cyclone interaction or exchange of water and mixing is one likely mechanism for decay of the swoddy anticyclone-cyclone eddy system. Water is exchanged between eddies and also drawn in from exterior regions along the jet structures between the eddy centers of opposite sign. This aspect is most clearly seen in SeaWiFS structure where different external level of chlorophyll *a* are drawn between eddies of opposite sign and wound around the centers of both cyclonic and anticyclonic eddies (see Figures 12c and 14).

3.2.6. Small-Scale Properties of Swoddy F90

[35] A temperature perturbation section of F90 (Figure 16a) was derived from the SeaSoar temperature profiles. Each SeaSoar profile (with values binned or interpolated to 1m levels) was smoothed with an 11 m running mean. The smoothed profiles were then subtracted from the original profiles to give a perturbation profile relative to the 11 m smoothing. The results show the swoddy core as a homogeneous region without temperature structure. In a similar manner, profiles of relative ADCP velocity (Figure 17), binned at 8 m intervals with 15 minute averages, show an inner core region without velocity structure. The zero for the ADCP profiles was fixed relative to a 100 m band centred near 150 m rather than the mean of the profile so that data spikes near the surface or resulting from weak signals at depth did not displace the plotted profiles. The ADCP cut shown is mainly north–south (see Figure 2c) and below the core (see region below <12.5°C isotherm) the relative east structure was generally to the east, south of the eddy center, and to the west in the north showing that below the core region the geostrophic currents were weaker at depth. Maximum shear is about 5 cm^{-1} per 100 m and not sufficient to cause instability in a gradient Richardson Number sense. Above the core (see region >13.0°C), the relative structure is even more marked and in general this will be directed in a sense such that the eddy surface currents decrease toward the surface above the core region (i.e., doming of the seasonal thermocline). Recently, it has been possible to relate the strength of Subtropical Front eddies or STORMS to an altimeter SLA signal (i.e., a transport of 10 Sv produced a SLA of ~10 cm) [*Pingree and Sinha*, 1998]. These eddies have their maximum currents near the sea surface, but in the case of swoddies and swoddy-like structures, the eddies have their maximum currents at about 100 m depth. The currents above this level are reduced as the thermocline is domed and so the altimeter does not see the full strength of the eddy, perhaps >0.5 for these small-scale eddies and there are also nonlinear surface effects (of about 10% of geostrophic effects) to consider. Further measurements of other swoddies will be necessary to relate the strength or azimuthal transport of swoddies to their altimeter SLA value. The swoddy core also appears stable as the Brunt-Vaisala frequency, although low, is measurable and significant (~0.3 cph) but the mean velocity shear near the core center is not sufficiently resolved from zero. The core region is likely to be periodically unstable, perhaps above the base, otherwise it would seem unlikely that the core properties would be so mixed well. In both Figures 16 and 17, isotherms have been drawn to show the core region near 12.9°C. The mixing in this region shows that there will be little or no production below about 60 m as light will be limiting. As expected, chlorophyll *a* fluorescence values are low in this region even when it is lifted nearer the surface, for example, at ~50 m near A in Figures 16a and 16b. The internal distribution of chlorophyll *a* (Figure 16b) is thus consistent with the physical small scale mixing structure and shows a distribution with respect to an anticyclonic eddy with increases of chlorophyll *a* above the core where the thermocline is domed

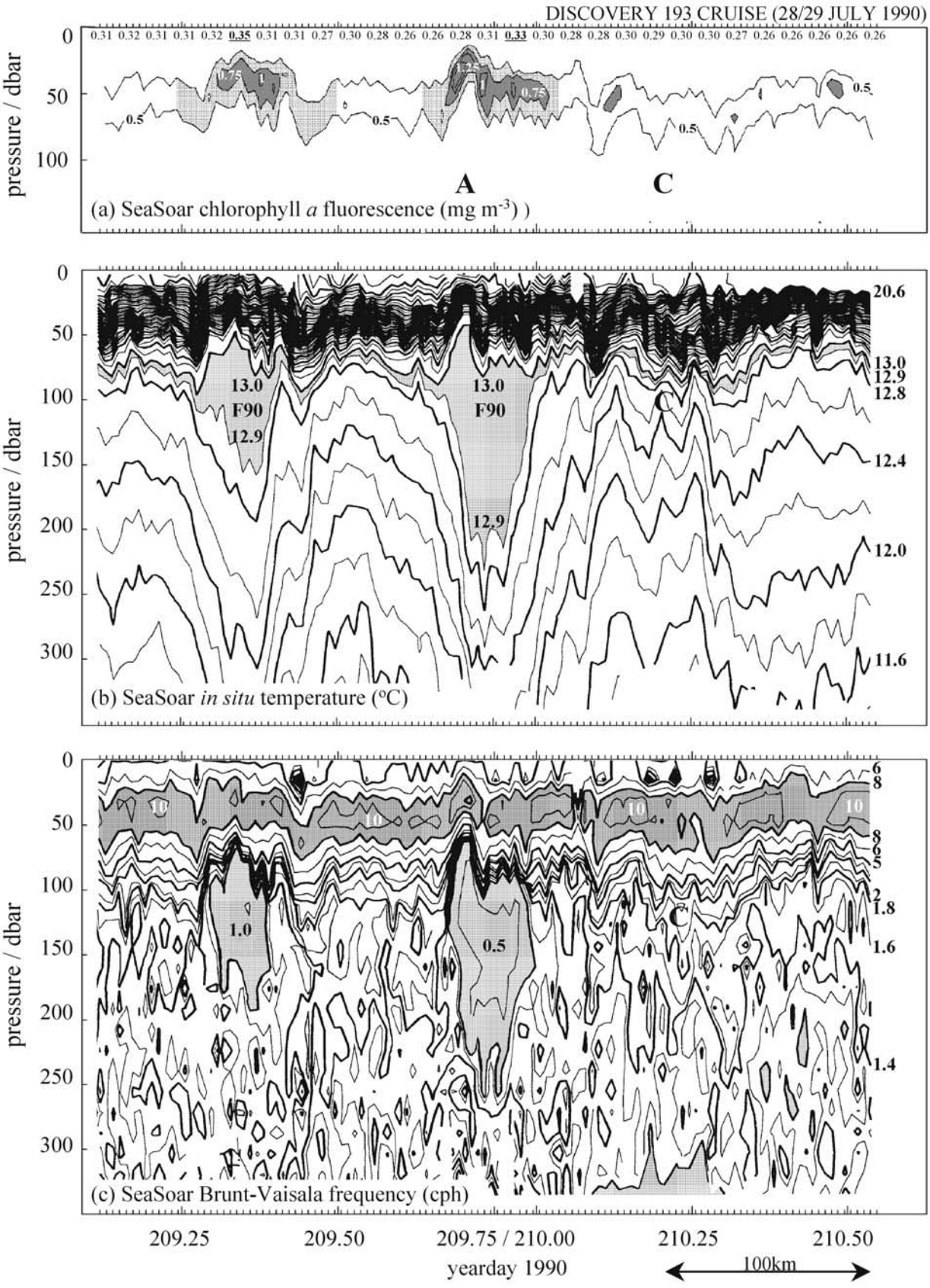
DISCOVERY 193 CRUISE (28/29 JULY 1990)
pressure / dbar
A
C
(a) SeaSoar chlorophyll *a* fluorescence (mg m^{-3}))
13.0
F90
12.9
(b) SeaSoar *in situ* temperature (ºC)
1.0
0.5
(c) SeaSoar Brunt-Vaisala frequency (cph)
209.25
209.50
209.75 / 210.00
210.25
210.50
yearday 1990
100km

upwards. Here, it is argued that there is a more favorable nutrient and light environment for phytoplankton growth. This region of increased chlorophyll *a* could also give this swoddy a remote sensing surface chlorophyll *a* signature, though no significant effect was observed in late summer 1998 (Figure 12c).

4. Summary and Conclusions

[36] The warm water extension of the Iberian Poleward Current around the NW corner of Spain and along the northern Spanish slope has been examined using the available AVHRR satellite archive (1979–2000) and a time series of January Sea Surface Temperature. This warm water extension has been called the Navidad as it generally starts near Christmas, becoming more fully developed in January. Winter warming in the Southern Bay of Biscay during marked Navidad years was found to be negatively correlated with values of the North Atlantic Oscillation (NAO) Index for the preceding months (November–December). Satellite images showing marked Navidad development along the Spanish slopes have been presented for 7 different years. Exceptional Navidad development and winter warming were observed in January 1990, January 1996, and January 1998 and extensive measurements were gathered for these three years. In years of exceptional warming, the warm water flow is not confined to the Portuguese and Spanish continental slopes but extends from the Subtropical Front in the South to the Polar Front or Faeroe-Shetland Channel, effectively forming a narrow warm eastern margin for Eastern North Atlantic Central Water. The continental slope "heat conductor" channels heat northward, collecting additional sources of warm ocean water as the flow increases poleward along the continental slope region. The climate consequences, milder winters for more northern latitudes, are significant. In a central region, the Celtic Sea for example, the additional heat flux in the slope region is equivalent to an extra month of summer heating. These effects are not just confined to the continental slope but are spread shelfward and oceanward by ocean margin exchange processes such as the production of eddies shed from the slopes into the ocean. Eddy-like structures transferring slope water to the ocean have now been observed from Lisbon, Portugal, to the Shetland Isles. During both January 1990 and January 1996, exceptional Navidad months, slope water eddies (swoddies) were observed in the SE corner of the Bay of Biscay, spreading the warm slope water influence into the ocean. The formation of all these structures could be related to abrupt slope topography. Long-term temperature data were also gathered for the Celtic Sea region to extend the longer term trends seen in the Navidad temperature time series to a central location along the ocean margin boundary. Over the last century, the central region has increased in temperature by nearly 1°C with the greatest rate of longer period change occurring near the last two decades of the 20th century.

[37] The second part of this study focuses on the summer structure of swoddies (F90) or swoddy-like eddies in the southern Bay of Biscay. These eddy types are examined in relation to their remote sensing sea surface signatures using IR, altimeter (combined TOPEX/Poseidon/ERS-2 data) and SeaWiFS data. Some of these eddies are redistributing their continental slope properties back into the ocean but they also have a local or intrinsic influence in the distribution of ocean properties. The interpretation of results hinges on the field measurements made during the Swoddy study of F90 in the summer of 1990, where it was shown that these anticyclonic eddies have a surface cool signature (they may also have smaller satellite cyclonic eddies associated with their exterior regions which have a warm surface signature). With this knowledge, the distribution of summer swoddy-like structures from 1979–2000 has been derived for the southern Bay of Biscay using the AVHRR archive. Their distribution showed that these eddies were markedly affected by topography in so far as that their centers could not move up or near the continental slope gradient (~1 km depth), being confined to water depths greater than about 3 km. The same cruise data showed that summer swoddy-like structure would be resolvable in altimeter data and this has been demonstrated for the eddy (AE6) observed in August 1998 in the Bay of Biscay, following the exceptional 1997–1998 winter Navidad. In addition, remote sensing SeaWiFS data, with much more spatial coverage than is possible with cruise data showed that the summer surface chlorophyll *a* response was largely one of a redistribution of ocean frontal-like properties by the surface eddy currents themselves. Although only one eddy was surveyed in August 1998, the remote sensing results showed similar structures associated with other eddies in the Bay of Biscay. This SeaWiFS surface chlorophyll *a* result is similar to that which was found for westward propagating Storm-like structures in the North Atlantic Ocean which perturb the ocean chlorophyll *a* near zonal frontal signal as it migrates northward with the productive season. In April, near 35°N west of the Mid-Atlantic Ridge, meridional protrusions with a zonal scale of a few hundred km (400–500 km) could be matched with altimeter sea level anomalies or westward propagating eddies [*Pingree et al.*, 1999a]. In the Bay of

Figure 15. (opposite) SeaSoar sections of (a) chlorophyll *a* fluorescence (mg Chl*a* m^{-3}, relative scale), (b) in situ temperature (°C), and (c) Brunt-Vaisala frequency (cph, relevant contours labeled) through the core of swoddy F90 (*Discovery* cruise 193, 28–29 July 1990; yeardays 209 and 210). A and C annotations indicate the main anticyclone (F90) and one of the associated cyclones, respectively. Yearday positions along the cruise track are shown in Figure 2d. The SeaSoar section covers approximately 300 CTD profiles along a track of ~420 km. In Figure 15a annotated top values correspond to chlorophyll values at the surface (maximum values underlined); dark shading highlights maximum levels above the two cuts of the swoddy core where the thermocline is domed upwards. In Figure 15b, the core of the eddy has also been highlighted with shading in the temperature range 12.9°–13.0°C. In Figure 15c, dark shading (>8 cph) highlights the maximum values of Brunt-Vaisala frequency in the seasonal thermocline and light shading (<1 cph) depicts the swoddy core with minimum values of <~0.5cph. The associated cyclone (C), where the isotherms are raised, has a core region with increased stability (Figure 15c) in the depth range ~80–180 m. The 100 km scale shown.

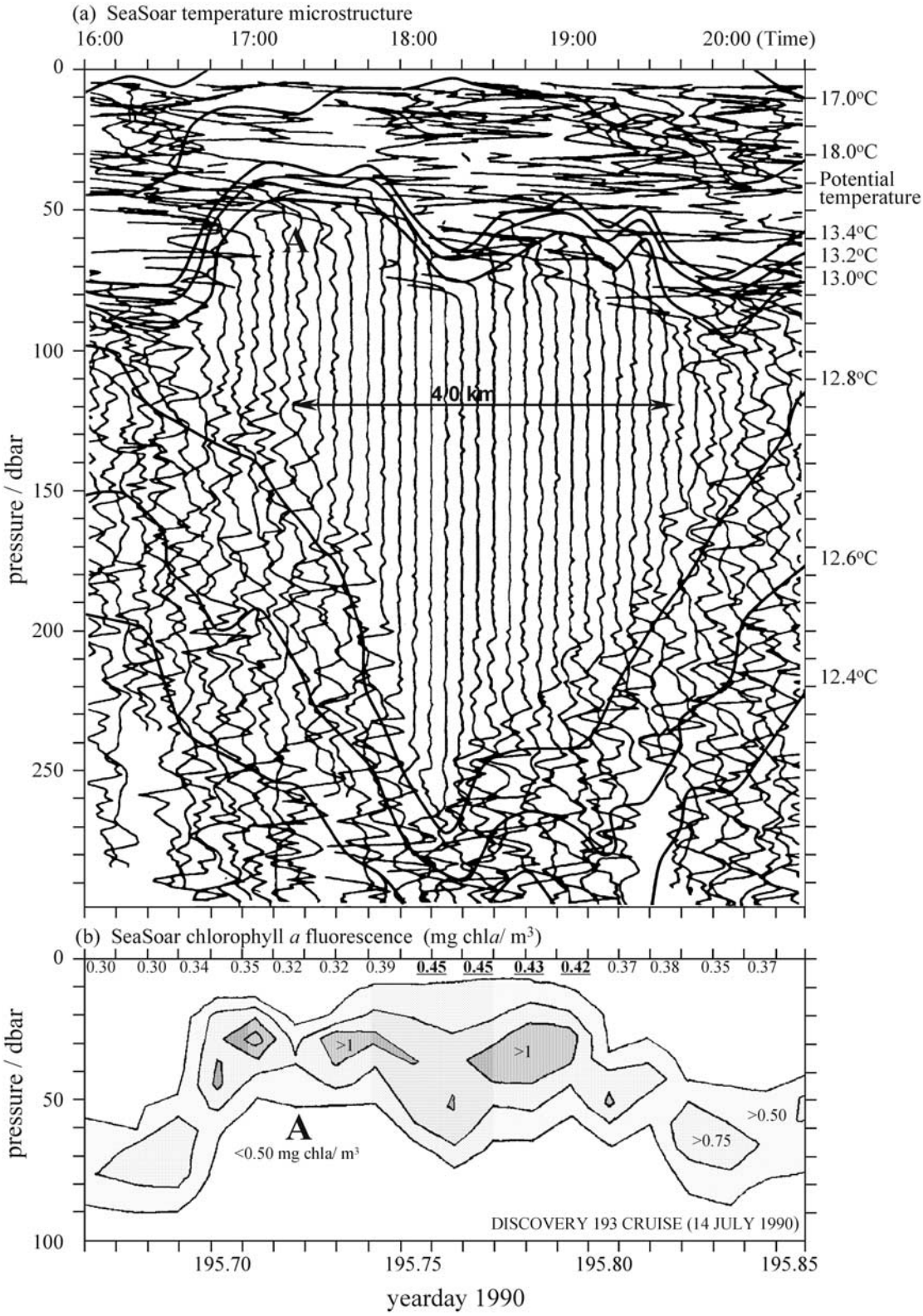

Figure 16. (a) SeaSoar temperature perturbation profiles through swoddy F90 on 14 July 1990 (yearday 195). Yearday positions along the cruise track are shown in Figure 2c. The section shows 45 perturbation profiles over a distance of about 75 km. Each profile is displaced by a scale of 0.01°C. Structures exceeding ±0.05°C (in the thermocline, for example) have not been plotted. Potential temperature isotherms from SeaSoar are superposed. 40 km scale shown in the eddy core. (b) The chlorophyll *a* fluorescence shows increased levels in the thermocline and at the surface (annotated top values) where the thermocline is domed upwards.

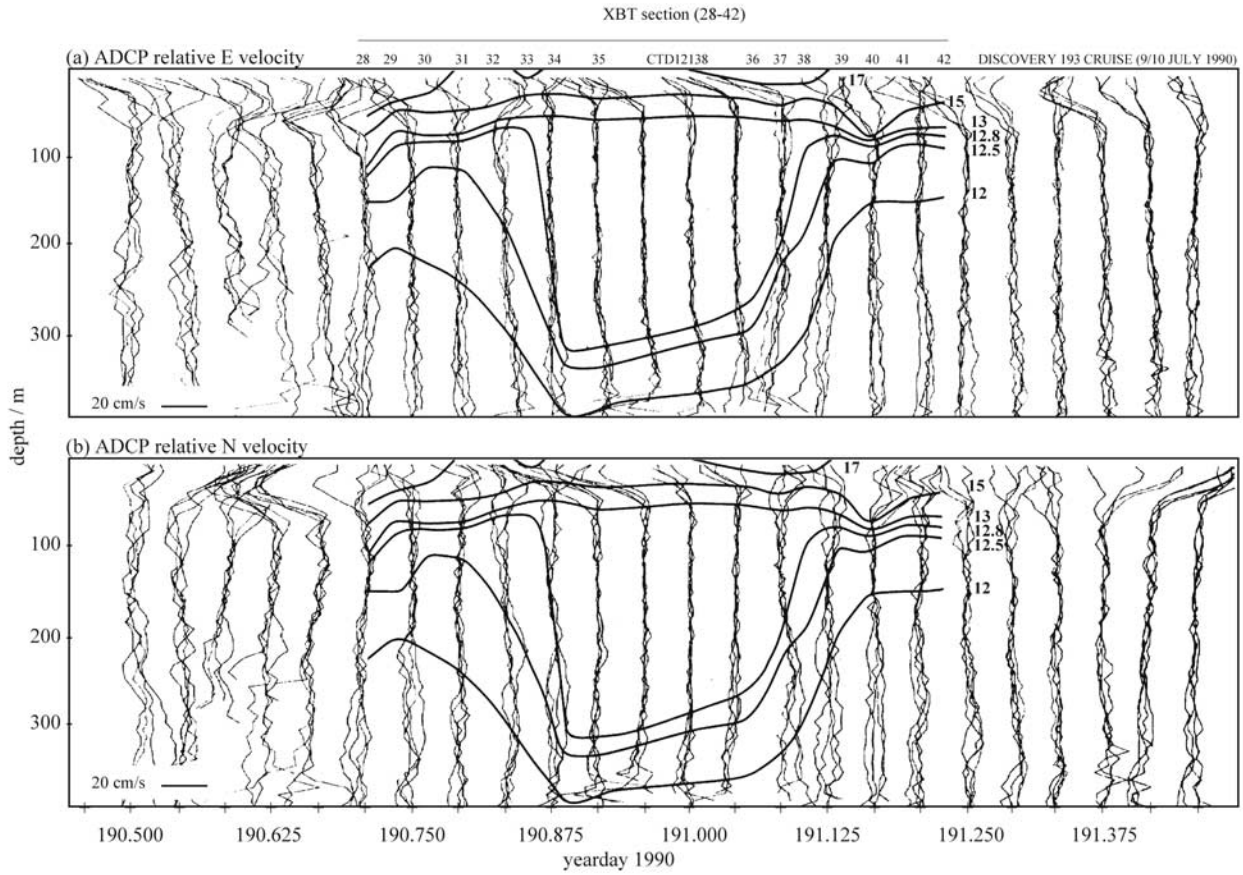

Figure 17. ADCP (a) east and (b) north relative velocity profiles obtained during the survey of swoddy F90 on 9–10 July 1990 (yeardays 190 and 191). The four profiles are plotted on a common scale that is then displaced by a scale of 20 cm s^{-1} for the next four profiles. Each set of four profiles gives an idea of the variability over an hour period. The ticks on the timescale show the zero for each set of four profiles. Yearday positions along the cruise track (*Discovery* cruise 193) are shown in Figure 2c. The location of the eddy core has been highlighted with an XBT section of in situ temperature (°C), which has been matched to the ADCP structure in time. The core of F90 is characterized by the reduced spatial velocity structure.

Biscay, the summer SeaWiFS chlorophyll *a* concentration at the center of the eddy near 45°N 6°W (AE6) was appraised against a time series (September 1997 to April 2001) of SeaWiFS chlorophyll *a* concentration for a central region. As with IR and altimeter data, continued ocean monitoring with SeaWiFS will allow interannual variations to be appraised. To take the interpretation of SeaWiFS structure further for the summer Biscay eddies, we have analyzed the small-scale structure of F90 from a SeaSoar survey of the eddy. A SeaSoar temperature perturbation section showed the swoddy core as a homogeneous region without temperature structure. ADCP profiles showed an inner core region with reduced velocity structure. Brunt-Vaisala frequency derived from SeaSoar CTD profiles gave eddy core values of about <1 cph, confirming low stability just below the seasonal thermocline. The physical structure of the eddy perturbs the distribution of properties in the euphotic layer and so has a control on the availability of nutrients and light energy necessary for phytoplankton growth. Increased levels of chlorophyll *a* above the eddy center where the thermocline is domed upwards can have an influence at the sea surface, which is remotely sensed. When this happens, SeaWiFS structure will show an elevated surface chlorophyll *a* region associated with the IR cooling and the altimeter positive sea level anomaly associated with the anticyclonic eddy core. By contrast, the summer cyclones associated with the anticyclone have a depressed thermocline and reduced levels of chlorophyll *a* and no SeaWiFS signature was found or anticipated. Overall, the aim has been to use and interpret the extensive remote sensing data coverage in terms of significant and selective measurements so that when ocean surface is sensed remotely we can also glean something of its subsurface or interior structure, and apply and quantify the results and interpretations given here over large spatial and temporal scales and with a resolution that is not possible from ship surveys.

[38] **Acknowledgments.** C. Garcia-Soto acknowledges a postdoctoral contract *RAMON Y CAJAL* from the Ministry of Science and Technology (MCyT) of Spain. A Joint Research grant of the British Council and the Project GIGOVI also supported this study. Sea Surface Temperature data of the NE Atlantic was kindly provided by M. Tremant

(Meteo-France). An extensive archive of AVHRR enhanced images (1979–2002) held at the Institute of Marine Science (IMS; Plymouth University) was made available by the Satellite Receiving Station at Dundee University (NERC-DSRS).

References

Alheit, J., and E. Hagen, Long-term climate forcing of European herring and sardine population, *Fish Oceanogr.*, *6*, 130–139, 1997.

Barston, A. G., and R. E. Livezey, Classification, seasonality and persistence of low-frequency atmospheric circulation patterns, *Mon. Weather Rev.*, *115*, 1083–1126, 1987.

British Oceanographic Data Centre (BODC), *General Bathymetric Chart of the Oceans; GEBCO 97 Digital Atlas*, Birkenhead, U.K., 1997.

Cayan, D. R., Latent and sensible heat flux anomalies over the northern oceans: The connection to monthly atmospheric circulation, *J. Clim.*, *5*, 354–369, 1992a.

Cayan, D. R., Latent and sensible heat flux anomalies over the northern oceans: Driving the sea surface temperature, *J. Phys. Oceanogr.*, *22*, 859–881, 1992b.

Centre de Météorologie (CMS), Bulletin mensuel rédigé par le Centre de Météorologie Spatiale, *Bull. Satmer*, *100*, 1–58, 1992.

Church, J. A., G. R. Cresswell, and J. S. Godfrey, The Leeuwin Current, in *Poleward Flows Along the Eastern Oceanic Boundaries, Coastal Estuarine Stud*, vol. 34, edited by S. J. Neshyba et al., pp. 230–252, Springer-Verlag, New York, 1989.

Cresswell, G. R., and T. J. Golding, Observations of a south flowing current in the southeast Indian Ocean, *Deep Sea Res., Part I*, *27*, 449–466, 1980.

Dickson, R. R., From the Labrador Sea to global change, *Nature*, *386*, 649–650, 1997.

Dickson, R. R., and D. G. Hughes, Satellite evidence of mesoscale eddy activity over the Biscay abyssal plain, *Oceanol. Acta*, *4*, 43–46, 1981.

Dickson, R. R., W. J. Gould, C. Griffiths, K. J. Medler, and E. M. Gmitrowicz, Seasonality in currents of the Rockall Channel, *Proc. R. Soc. Edinburgh, Ser. B*, *88*, 103–125, 1986.

Dickson, R. R., J. Lazier, J. Meincke, P. Rhines, and J. Swift, Long-term coordinated changes in the convectivity activity of the North Atlantic, *Prog. Oceanogr.*, *38*, 241–295, 1996.

Fernández, E., J. Cabal, J. L. Acuña, A. Bode, A. Botas, and C. Garcia-Soto, Plankton distributions across a slope current-induced front in the southern Bay of Biscay, *J. Plankton Res.*, *15*, 619–641, 1993.

Fiuza, A. F. G., M. Hammann, I. Ambar, G. Diaz del Río, N. González, and J. M. Cabanas, Water masses and their circulation in the western Iberian coastal ocean during May 1993, *Deep Sea Res., Part I*, *45*, 1127–1160, 1998.

Frouin, R., A. F. G. Fiúza, I. Ambar, and T. J. Boyd, Observations of a poleward surface current off the coasts of Portugal and Spain during winter, *J. Geophys. Res.*, *95*, 679–691, 1990.

Garcia-Soto, C., and R. D. Pingree, Late autumn distribution and seasonality of chlorophyll-*a* at the shelf-break/slope region of the Armorican and Celtic Shelf, *J. Mar. Biol. Assoc. U.K.*, *78*, 17–33, 1998.

Garcia-Soto, C., N. C. H. Halliday, S. B. Groom, A. Lavín, and S. H. Coombs, Satellite imagery, hydrography and plankton distributions off NW Spain in April–May 1991, *ICES CM Pap. Rep.*, *17*, 10 pp., 1991.

Garcia-Soto, C., E. Fernández, R. D. Pingree, and D. S. Harbour, Evolution and structure of a shelf coccolithophore bloom in the western English Channel, *J. Plankton Res.*, *17*, 2011–2036, 1995.

Gould, W. J., J. Loynes, and J. Backhaus, Seasonality in slope current transports NW of Shetland, *ICES CM Pap. Rep.*, *7*, 7 pp., 1985.

Griffiths, A. F., and R. W. Pearce, Satellite images of an unstable warm eddy derived from the Leeuwin Current, *Deep Sea Res., Part I*, *32*, 1371–1380, 1985a.

Griffiths, A. F., and R. W. Pearce, Instability and eddy pairs on the Leeuwin Current south of Australia, *Deep Sea Res., Part I*, *32*, 1511–1534, 1985b.

Hagen, E., and G. Schmager, On mid latitude air pressure variations and related SSTA fluctuations in the tropical/subtropical Northern Atlantic from 1957 to 1974, *Z. Meteorol.*, *41*, 176–190, 1991.

Haynes, R., and E. D. Barton, A poleward flow along the Atlantic coast of the Iberian peninsula, *J. Geophys. Res.*, *95*, 11,425–11,441, 1990.

Holligan, P. M., T. Aarup, and S. B. Groom, The North Sea Satellite Colour Atlas, *Cont. Shelf Res.*, *9*, 665–765, 1989.

Hurrell, J. W., Decadal trends in the North Atlantic Oscillation: Regional temperatures and precipitation, *Science*, *269*, 676–679, 1995.

Hurrell, J. W., Influence of variations in extratropical wintertime teleconnections on Northern Hemisphere temperature, *Geophys. Res. Lett.*, *23*, 6665–6668, 1996.

International Council for the Exploration of the Sea (ICES), Monthly means of surface temperature and salinity for areas of the North Sea and northeastern North Atlantic in 1967, 15 pp., Charlottenlund, Denmark, 1971.

Koutsikopoulos, C., and B. Le Cann, Physical processes and hydrological structures related to the Bay of Biscay anchovy, *Sci. Mar.*, *60*, 9–19, 1996.

Koutsikopoulos, C., P. Beillois, C. Leroy, and F. Taillefer, Temporal trends and spatial structures of the sea surface temperature in the Bay of Biscay, *Oceanol. Acta*, *21*, 335–344, 1998.

Kushnir, Y., Interdecadal variations in North Atlantic sea surface temperature and associated atmospheric conditions, *J. Clim.*, *7*, 141–157, 1994.

Lavín, A., and J. M. Cabanas, Area 4 (Bay of Biscay and Eastern Atlantic) Spanish Report. Annex N of the Report of the Working Group on Oceanic Hydrography, *ICES CM Pap. Rep.*, *6*, 110–117, 2001.

Le Traon, P. Y., and F. Ogor, ERS-1/2 orbit error improvement using TOPEX-Poseidon: The 2 cm challenge, *J. Geophys. Res.*, *103*, 8045–8057, 1998.

Levitus, S., J. Antonov, T. P. Boyer, and C. Stephens, Warming of the world oceans, *Science*, *287*, 2225–2229, 2000.

Loeng, H., J. Blindheim, B. Ådlandsvik, and G. Ottersen, Climatic variability in the Norwegian and Barents Seas, *ICES Mar. Sci. Symp.*, *195*, 52–61, 1992.

Manley, G., Central England temperatures: Monthly means 1659–1973, *Q.J.R. Meteorol. Soc.*, *100*, 389–405, 1974.

Mann, M. E., R. S. Bradley, and M. K. Hughes, Northern Hemisphere temperatures during the past millenium: Inferences, uncertainties, and limitations, *Geophys. Res. Lett.*, *26*, 759–762, 1999.

Marshall, J., Y. Kushnir, D. Battisti, P. Chang, A. Czaja, R. Dikson, J. Hurrell, M. McCartney, R. Saravanan, and M. Visvack, North Atlantic climate variability: Phenomena, impacts and mechanisms, *Int. J. Climatol.*, *21*, 1863–1898, 2001.

Neshyba, S. J., C. N. K. Mooers, R. L. Smith, and R. T. Barber, (Eds), *Poleward Flows Along Eastern Ocean Boundaries, Coastal and Estuarine Stud.*, vol 34, 374 pp., AGU, Washington, D.C., 1989.

Pearce, A. F., and R. W. Griffiths, The mesoscale structure of the Leeuwin Current: A comparison of laboratory models and satellite imagery, *J. Geophys. Res.*, *96*, 16,739–16,757, 1991.

Pingree, R. D., The advance and retreat of the thermocline on the continental shelf, *J. Mar. Biol. Assoc. U.K.*, *55*, 965–974, 1975.

Pingree, D. R., The physical oceanography of the Celtic Sea and English Channel, in *The Northwest European Shelf Seas: The Sea-Bed and the Sea in Motion*, edited by F. T. Banner, M. B. Collins, and K. S. Massie, chap. 13, pp. 415–465, Elsevier Sci., New York, 1980.

Pingree, R. D., Some applications of remote sensing to studies in the Bay of Biscay, Celtic Sea and English Channel, in *Remote Sensing of Shelf Sea Hydrodynamics*, edited by J. C. J. Nihoul, pp. 287–315, Elsevier Sci., New York, 1984.

Pingree, R. D., Flow of surface waters to the west of the British Isles and in the Bay of Biscay, *Deep Sea Res., Part II*, *40*, 369–388, 1993.

Pingree, R. D., Winter warming in the Southern Bay of Biscay and Lagrangian eddy kinematics from a deep-drogued Argos buoy, *J. Mar. Biol. Assoc. U.K.*, *74*, 107–128, 1994a.

Pingree, R. D., Physical processes: slope ocean boundary exchange, in *Ocean Margin Exchange* (*OMEX*), *First Annual Report* (*August 1994*), Comm. of the Eur. Union, Brussels, 1994b.

Pingree, R. D., The eastern Subtropical Gyre (North Atlantic): Flow rings recirculation structure and subduction, *J. Mar. Biol. Assoc. U.K.*, *77*, 573–624, 1997.

Pingree, R. D., Ocean structure and climate (eastern North Atlantic): In situ measurements and remote sensing (altimeter), *J. Mar. Biol. Assoc. U.K.*, *81*, 1–22, 2002.

Pingree, R. D., and B. Le Cann, Celtic and Armorican slope and shelf residual currents, *Prog. Oceanogr.*, *23*, 303–338, 1989.

Pingree, R. D., and B. Le Cann, Structure, strength and seasonality of the slope currents in the Bay of Biscay region, *J. Mar. Biol. Assoc. U.K.*, *70*, 857–885, 1990.

Pingree, R. D., and B. Le Cann, Three anticyclonic slope water oceanic eddies (swoddies) in the southern Bay of Biscay in 1990, *Deep Sea Res., Part I*, *39*, 1147–1175, 1992a.

Pingree, R. D., and B. Le Cann, Anticyclonic eddy X91 in the Southern Bay of Biscay, May 1991 to February 1992, *J. Geophys. Res.*, *97*, 14,353–14,367, 1992b.

Pingree, R. D., and B. Le Cann, A Shallow MEDDY (a SMEDDY) from the secondary Mediterranean salinity maximum, *J. Geophys. Res.*, *98*, 20,169–20,185, 1993.

Pingree, R. D., and B. Sinha, Dynamic topography (ERS-1/2 and Seatruth) of Subtropical Ring (STORM 0) in the Storm Corridor (32–34°N, Eastern Basin, North Atlantic Ocean), *J. Mar. Biol. Assoc. U.K.*, *76*, 351–376, 1998.

Pingree, R. D., C. Garcia-Soto, and B. Sinha, Position and structure of the SubTropical/Azores Front region from combined Lagrangian and remote sensing (IR/altimeter/SeaWiFS) measurements, *J. Mar. Biol. Assoc. U.K.*, *79*, 769–792, 1999a.

Pingree, R. D., B. Sinha, and C. R. Griffiths, Seasonality of the European

slope current (Goban Spur) and ocean margin exchange, *Cont. Shelf Res.*, *19*, 929–975, 1999b.

Sánchez, F., and J. Gil, Hydrographic mesoscale structures and Poleward Current as a determinant of hake (Merluccius merluccius) recruitment in the southern Bay of Biscay, *ICES CM Pap. Rep.*, *57*, 152–170, 2000.

Urrutia, J., C. Garcia-Soto, Sistemas frontales costeros del Golfo de Vizcaya detectados mediante radiometría infra-roja (NOAA), in *III Reunión Científica del Grupo de Trabajo en Teledetección*, edited by C. Antón Pacheco and J. L. Labrandero, pp. 317–325, Serv. de Publ. del Minist. de Ind. y Energía, Inst. Tecnol. y Geominero, Madrid, Spain, 1990.

Visbeck, M., J. Hurrell, and Y. Kushnir, First International Conference on the North Atlantic Oscillation (NAO): Lessons and Challenges for CLIVAR, *CLIVAR Exch.*, *6*, 24–25, 2001.

R. D. Pingree, Institute of Marine Sciences (IMS), Plymouth University, Drake Circus, Plymouth PL4 8AA, UK.

C. Garcia-Soto and L. Valdés, Centro Oceanográfico de Santander, Instituto Español de Oceanografía (IEO), Ministerio de Ciencia y Tecnología (MCyT); Promontorio de San Martin s/n, 39004 Santander, Spain. (carlos.soto@st.ieo.es)